UNIVERSIDADE ESTADUAL PAULISTA – UNESP

CÂMPUS DE JABOTICABAL

MODELAGEM AGROMETEOROLÓGICA PARA PREVISÃO DE PRODUTIVIDADE DE AÇAIZEIRO

José Reinaldo da Silva Cabral de Moraes

Engenheiro Agrônomo

2017

UNIVERSIDADE ESTADUAL PAULISTA – UNESP

CÂMPUS DE JABOTICABAL

MODELAGEM AGROMETEOROLÓGICA PARA PREVISÃO DE PRODUTIVIDADE DE AÇAIZEIRO

José Reinaldo da Silva Cabral de Moraes

Orientador: Prof. Dr. Glauco de Souza Rolim

Dissertação apresentada à Faculdade de Ciências Agrárias e Veterinárias – UNESP, Câmpus de Jaboticabal, como parte das exigências para a obtenção do título de Mestre em Agronomia (Produção Vegetal).

2017

M827m Moraes, José Reinaldo da Silva Cabral de
Modelagem agrometeorológica para previsão de produtividade de açaizeiro / José Reinaldo da Silva Cabral de Moraes. – – Jaboticabal, 2017
xii, 78 p. : il. ; 29 cm

Dissertação (mestrado) - Universidade Estadual Paulista, Faculdade de Ciências Agrárias e Veterinárias, 2017
Orientador: Glauco de Souza Rolim
Banca examinadora: Lucieta Guerreiro Martorano, Maria do Socorro Padilha de Oliveira
Bibliografia

1. Amazônia. 2. Dados em GRID. 3. *Euterpe Oleracea*, 4. Modelos de previsão. I. Título. II. Jaboticabal-Faculdade de Ciências Agrárias e Veterinárias.

CDU 633:582.521.11

Ficha catalográfica elaborada pela Seção Técnica de Aquisição e Tratamento da Informação – Diretoria Técnica de Biblioteca e Documentação - UNESP, Câmpus de Jaboticabal.

UNIVERSIDADE ESTADUAL PAULISTA

Câmpus de Jaboticabal

CERTIFICADO DE APROVAÇÃO

TÍTULO DA DISSERTAÇÃO: MODELAGEM AGROMETEOROLÓGICA PARA PREVISÃO DE PRODUTIVIDADE DE AÇAIZEIRO

AUTOR: JOSÉ REINALDO DA SILVA CABRAL DE MORAES
ORIENTADOR: GLAUCO DE SOUZA ROLIM

Aprovado como parte das exigências para obtenção do Título de Mestre em AGRONOMIA (PRODUÇÃO VEGETAL), pela Comissão Examinadora:

Prof. Dr. GLAUCO DE SOUZA ROLIM
Departamento de Ciências Exatas / FCAV / UNESP - Jaboticabal

Pesquisadora Dra. MARIA DO SOCORRO PADILHA DE OLIVEIRA - VIDEOCONFERÊNCIA
Embrapa Amazônia Oriental / EMBRAPA / Belém/PA

Pesquisadora Dra. LUCIETA GUERREIRO MARTORANO - VIDEOCONFERÊNCIA
Embrapa Amazônia Oriental / EMBRAPA / Santarém/PA

Jaboticabal, 31 de julho de 2017

DADOS CURRICULARES DO AUTOR

JOSÉ REINALDO DA SILVA CABRAL DE MORAES- Nascido em Castanhal, Pará, no dia 27 de abril de 1992, filho de José da Silva Moraes e Lilia da Silva Cabral de Moraes, cursou o ensino fundamental no colégio estadual Aristedes Santa Rosa, no município de Inhangapi, Pará, e o ensino médio no Instituto de Educação Darwin, no município de Castanhal, Pará, tendo finalizado no ano de 2009. Ingressou no ensino superior no ano de 2010 no curso de Engenharia Agronômica pela Universidade Federal Rural da Amazônia (UFRA), Campus Belém, Pará, obtendo o título de Engenheiro Agrônomo em janeiro de 2016. Durante a graduação foi bolsista do Programa de Educação Tutorial (PET) Agronomia, sob a tutoria do Prof. Dr. Carlos Augusto Cordeiro Costa por quatro anos. Realizou iniciação científica na Empresa Brasileira de Pesquisa Agropecuária (EMBRAPA) Amazônia Oriental, também durante quatro anos, na área de Agrometeorologia, sob a orientação da pesquisadora Dra. Lucieta Guerreiro Martorano. Realizou durante um ano estágio curricular na área de agrometeologia e modelagem na UFRA, sob a orientação do Prof. Dr. Paulo Jorge de Oliveira Ponte de Souza, onde veio a desenvolver seu trabalho de conclusão de curso, com calibração do modelo DSSAT para o feijão caupi. Durante esses períodos, colaborou na elaboração de eventos científicos, palestras, workshop e publicação de resumos e artigos indexados. Em agosto de 2015, iniciou o curso de Mestrado em Agronomia, no Programa de Produção Vegetal, na área de Modelagem Agrometeorológica, pela Universidade Estadual Paulista "Júlio de Mesquita Filho" – Campus de Jaboticabal, São Paulo, no grupo de pesquisa Group of Agrometeorological Studies (GAS), sob a orientação do Prof. Dr. Glauco de Souza Rolim. Durante o mestrado realizou pesquisas com foco em modelagem agrometeorológica para o cultivo do açaizeiro, a partir de dados em grid. Em julho de 2017, submeteu-se à banca examinadora para obtenção do título de Mestre em Agronomia.

"Hoje, ainda almejamos saber porque estamos aqui e de onde viemos. O desejo profundo da humanidade pelo conhecimento é justificativa suficiente para nossa busca contínua".

Stephen Hawking

Aos meus pais José da Silva Moraes e Lilia da Silva Cabral de Moraes, pela educação e amor que sempre me proporcionaram, nunca deixando nada de essencial faltar para que eu pudesse trilhar meu caminho profissional.

A vocês,

DEDICO!

Ao meu Avôs Sebastião de Oliveira Moraes e Antônio Terra da Trindade (*In memorian*).

OFEREÇO!

AGRADECIMENTOS

A Deus, por sempre me acompanhar, iluminando meus caminhos e minhas escolhas, me dando força, saúde e paz, para que eu pudesse alcançar e realizar meus sonhos para atingir metas pessoal e profissional.

À Universidade Federal Rural da Amazônia, que proporcionou minha formação como Engenheiro Agrônomo. Ao Programa de Pós-Graduação em Agronomia (Produção Vegetal) da Universidade Estadual Paulista "Júlio de Mesquita Filho" Faculdade de Ciências Agrárias e Veterinárias, Campus de Jaboticabal, pela oportunidade de realização do mestrado e ao Conselho Nacional de Desenvolvimento Científico e Tecnológico (CNPq), pela concessão de bolsa durante o período de realização do curso.

Aos meus familiares, em especial aos meus pais, José Moraes e Lilia Moraes e minha irmã Liliane Moraes, bem como a Josi Moraes pelo amor, carinho e dedicação.

À minha avó paterna, Raimunda Monteiro da Silva Moraes e materna, Nazaré Cabral, meu avô paterno, Sebastião de Oliveira Moraes (*In memorian*) e meus avós de coração, Maria das Dores Terra e Antônio Terra da Trindade (*In memorian*), pelos ensinamentos e carinhos frequentes.

Aos meus tios, em especial, Reinaldo Moraes e Ieda Terra, pela força, carinho, confiança e apoio durante o período que vivi com eles em Belém.

Aos meus sobrinhos, Ana Beatriz, Joaquim e Julia, que chegaram nessa vida para trazer alegria a toda minha família e que os tenho como filhos e minha nova sobrinha Elissa, que vem trazendo muito amor e carinho.

Ao meu orientador Prof. Dr. Glauco de Souza Rolim, por quem eu tenho muita admiração e respeito, meus sinceros agradecimentos pelos ensinamentos e votos de confiança durante o mestrado.

À minha orientadora Lucieta Guerreiro Martorano, pela confiança e ensinamentos durante minha graduação e posterior, inclusive na pós-graduação.

À Embrapa Amazônia Oriental, em especial aos pesquisadores Dra. Socorro Padilha e Dr. João Tomé, pela concessão dos dados de campo para a realização dessa pesquisa.

Aos meus amigos científicos e de coração do GAS, Taynara Valeriano, Lucas Aparecido, Victor Moreto, Kamila Meneses, Juliana, João e Clayson.

Meus agradecimentos aos funcionários do departamento de ciências exatas em especial aos amigos Carlão, Vanessa, Zezé, Shirlei e Adriana. Ao professor Newton e amigos Bruna, Gustavo, Daniel e Mara.

Registro também meus agradecimentos aos companheiros do Galáticos futebol, amigos que conquistei durante o mestrado.

Aos colegas que já terminaram suas metas em Jaboticabal e foram trilhar novos caminhos, Francisco Carlos, Flávio José e Raphael Leone.

Ao meu amigo, Daniel Pinheiro, pela agradável convivência durante minha estadia em Jaboticabal, pelas horas de conversas em momentos difíceis e pelo acolhimento e companheirismo durante meu mestrado. A minha querida amiga, Aline Barbosa pelos anos de amizade, conversas, apoio e confiança durante esse período.

Os colegas do Laboratório de Agrometeorologia da Embrapa Amazônia Oriental pelo carinho, amizade e parceria durante a iniciação científica que muito contribuiu para minha formação profissional.

E a todos que de certa forma contribuíram para minha formação de vida e profissional.

SUMÁRIO

MODELAGEM AGROMETEOROLÓGICA PARA PREVISÃO DE PRODUTIVIDADE DE AÇAIZEIRO

RESUMO

Modelos agrometeorológicos para a previsão da produtividade permitem a avaliação quantitativa de elementos meteorológicos com as variáveis fenológicas e produtividade, auxiliando no planejamento de safras agrícolas para otimizar estratégias e tomada de decisão. Na região amazônica, mais precisamente no estado do Pará, concentram-se as maiores produções de açaí no Brasil, entretanto a sazonalidade na produção, influenciada principalmente pelo clima que altera fortemente o preço do produto, tornando-se preocupante para toda cadeia produtiva. Portanto analisar o desempenho de modelos de circulação geral (GSM), que possam representar as condições de tempo e clima na região é de grande importância para a sustentabilidade da produção. Objetivou-se avaliar os dados de temperatura do ar (T) e precipitação (P) provenientes do modelo do European Center for Medium-Range Weather Forecast (ECMWF) e desenvolver modelos agrometeorológicos para a previsão da produtividade em cultivos de açaizeiro em Tomé Açu, Pará. Dados de T e P de estações meteorológicas de superfícies foram estimados por regressão linear usando dados em grid do (ECMWF), correspondendo ao período de 1990 a 2014, separando-se em escala decendial e mensal. Com base nos dados estimados foram testados e ajustados modelos de regressão linear múltipla para prognosticar a produtividade em dois tipos de cultivo de açaizeiro. Buscou-se maximizar a data para antecipação da previsão. A variável dependente foi à produtividade da cultura, enquanto que, as variáveis independentes foram os elementos meteorológicos decendiais e mensais, para cultivos irrigado (CI) e não irrigado (CNI). O ECMWF tende a superestimar precipitação pluvial na estação seca e subestimá-lo na estação chuvosa. A região noroeste da Amazônia é caracterizada como a área de maior oferta de P, mas com menores desempenhos do modelo com R^2 inferior a 0,18. O modelo ECMWF apresentou alto desempenho (R^2> 0,60) ao estimar P em escala mensal e desempenho médio (R^2<0,60) ao estimar T em período mensal e decendial. As maiores precisões do ECMWF foram nas áreas antrópicas no sudeste e nordeste da região amazônica, precisamente onde localizam-se os pólos de produção de açaí. A fase de folha madura e emissão de espata, para CI e CNI foram as mais sensíveis às condições climáticas. As maiores produções de frutos por planta ocorreram nos meses de novembro e dezembro, nos dois sistemas de cultivo. As observações apontaram produtividades que variaram entre 16.500 kg ha^{-1} em CI e 7.500 kg ha^{-1} em CNI. Os modelos agrometeorológicos foram acurados com valores máximos de MAPE de 0,01 no CI e 1,12 no CNI. Foi possível a previsão da produtividade em média de 6 a 9 meses antes da colheita, em abril, maio, novembro e dezembro no CI e em janeiro, maio, junho, agosto, setembro e novembro para CNI.

PALAVRAS-CHAVE: amazônia, dados em GRID, *Euterpe Oleracea*, modelos de previsão.

AGROMETEOROLOGICAL MODELING FOR FORECASTING AÇAI YIELD

ABSTRACT

Agrometeorological models for yield prediction allow the quantitative evaluation of the meteorological elements with the phenological variables and yield, aiding in the planning of agricultural crops and in the optimization of decision making. In the Amazon region, more precisely in the Pará State, the largest açai production is found in Brazil. However, seasonality in production, influenced mainly by the climate, is strongly affecting the price of the product, causing concern for the entire production chain. Therefore, evaluating the performance of general circulation models (GSM), which may represent the weather and climate conditions in the region, is of great importance for the sustainability of production. The objective of this study was to evaluate the air temperature (T) and precipitation (P) data from the European Center for Medium-Range Weather Forecast (ECMWF) model and to develop agrometeorological models for yield prediction in açai crop in Tomé Açu, Pará. T and P of meteorological stations of surfaces were estimated by linear regression using grid data of the ECMWF, from the period 1990 to 2014, separating in 10-day period and monthly scale. Based on the estimated data, multiple linear regression models were tested and adjusted to predict yield in two types of açai culture. We seek to maximize the date for anticipation of the forecast. The dependent variable was crop yield, while the independent variables were meteorological elements for irrigated system (IRRS) and rainfed system or unirrigated (RAINF). The ECMWF tends to overestimate rainfall in the dry season and to underestimate it in the rainy season. The northwest region of Amazonia is characterized as the area of highest rainfall supply (P), but with lower performances of the model with R^2 less than 0.18. The ECMWF model presented a high performance (R^2> 0.60) when estimating P on monthly scale and mean performance (R^2<0.60) when estimating T in monthly and 10-day period. The most important ECMWF accuracies were in the anthropic areas in the southeast and northeast of the Amazon region, precisely where the açai production poles are located. The phase of leaf maturation and emission of the spathe, for both IRRS and RAINF, were the variables that were most sensitive to climate conditions. The greatest fruit production occurred in November and December in each cultivation system, and production ranged from 7.500 kg ha^{-1} in the RAINF to 16.500 kg ha^{-1} in the IRRS. The accuracy of the agrometeorological models, using maximum values for average absolute percent error (MAPE), was 0.01 in the IRRS and 1.12 in the RAINF. Using these models production was predicted approximately 6 to 9 months before the harvest, in April, May, November, and December in the IRRS, and January, May, June, August, September, and November for the RAINF.

KEYWORDS: amazon, data in GRID, *Euterpe Oleracea*, prediction models

CAPÍTULO 1 – CONSIDERAÇÕES GERAIS

1 Introdução

O açaizeiro (*Euterpe oleracea* Mart) é uma cultura agrícola de importância na região norte do Brasil, sendo um fruto típico e popular da região amazônica (Oliveira et al., 2000). O clima é o principal fator de desenvolvimento e produtividade da cultura. Nos locais de ocorrência natural e de cultivo na Amazônia brasileira, a espécie pode ser encontrada em áreas submetidas aos tipos climáticos Afi, Ami e Awi, (classificação de Köppen). Contudo, sua população nativa concentra-se no tipo Afi, caracterizado por totais pluviométricos anuais superiores a 2.000 mm com distribuição uniforme e meses de menor precipitação pluvial com total mensal sempre superior a 60 mm (NASCIMENTO e HOMMA, 1984).

A melhor forma de sintetizar quantitativamente os efeitos das condições climáticas no desenvolvimento e produtividade do açaizeiro é por meio de modelos de cultivos. O uso de modelos agrometeorológicos permite conhecer previamente as safras agrícolas. Por meio de modelos de previsão, pode-se auxiliar no planejamento agrícola e avaliar as condições climáticas que podem limitar ou potencializar a expressão genética em termos de produtividade potencial, identificando as condicionantes de variáveis atmosféricas que possam causar perdas de produção e buscar soluções estratégicas para tomada de decisão.

Contudo, modelos de previsão da produtividade são escassos na literatura, uma vez que os mais usuais, pela facilidade e manuseio, são os de estimação. Moreto e Rolim (2015) definem a previsão como o ato de estimar para o futuro, com os dados disponíveis atuais prever um fenômeno que ainda não ocorreu. Diferentemente da estimação, que, a partir de dados atuais simula uma condição também atual. Mas, para que se possa desenvolver e avaliar as variáveis empregadas nos modelos agrometeorológicos, se faz necessário o aporte de dados meteorológicos, disponibilizados por estações de superfície automáticas ou convencionais. Segundo Pereira et al. (2002) o Brasil por suas dimensões continentais ainda não apresenta uma rede de estações meteorológicas que atenda às suas necessidades, sendo que em áreas mais desenvolvidas há um maior número do que em outras mais remotas.

Surge, então, a necessidade de alternativas para a fonte desses dados. Uma opção consistente é a utilização de dados meteorológicos provenientes de Modelos de Circulação Geral (GCM), sendo ferramentas importantes para previsões climáticas e pesquisa sobre mudanças no clima global (MIRIN e SAWYER, 2005; NAKAEGAWA et al., 2013; SATOH, 2014). Atuando como um dos componentes mais importantes de um modelo de sistema terrestre (WANG et al., 2017), sendo significativamente melhorados nas últimas décadas (REICHLER e KIM 2008).

Para realizar a simulação climática, os GCM geralmente precisam ser integrados por vários anos ou décadas (WANG et al., 2014), combinando informações de diversas fontes, superfície, oceanos, sensoriamento remoto e fazendo estimações e previsões das condições meteorológicas separando a superfície e a atmosfera do planeta em um grid de 3 dimensões (BECHTOLD et al., 2008). Este método tem sido usado cada vez mais desde o final de 1980 (CESS et al., 1989; GATES et al., 1999; LAMBERT e BOER, 2001), especialmente para a avaliação das mudanças climáticas, desempenhando um papel importante para aquisição de informações climatológicas em áreas remotas do globo terrestre.

Com base no exposto objetivou-se avaliar os dados provenientes do modelo ECMWF e desenvolver modelos agrometeorológicos de previsão da produtividade para cultivos de açaizeiro no estado do Pará.

1.1 REVISÃO DE LITERATURA

1.1.1 Modelagem agrometeorológica

O uso de modelos agrometeorológicos de previsão de produtividade permite a ligação quantitativa dos elementos meteorológicos com a fenologia e a produtividade, auxiliando também no planejamento da atividade no campo. Esses modelos consideram a influência de elementos climáticos sobre a produtividade da cultura, funcionando como um medidor de eficiência. Os métodos utilizados para estabelecer a relação planta-clima variam desde a simples correlação, até modelos complexos, ou seja, funções de produção que podem considerar diferentes parâmetros envolvidos no sistema produtivo (PICINI, 1999).

Rolim et al. (2008) ressaltam que os modelos de crescimento e desenvolvimento de culturas constituem uma conveniente forma de sintetizar informações das condições climáticas, fisiologia, níveis tecnológicos de produção, solos e até mesmo de mercado, tornando possível a simulação da fenometria da produtividade e qualidade dos produtos agrícolas.

No Brasil os trabalhos com modelagem agrometeorológica vêm sendo realizados para estimação e previsão de produtividades agrícolas de culturas como o citros, trigo, cana- de-açúcar, arroz, café, entre outras. Por exemplo, Monteiro et al. (2013) avaliaram um sistema de estimativa de produtividade da cultura do arroz no Brasil, com base em modelos agrometeorológicos simples e no nível tecnológico dos sistemas produtivos, onde constataram que o modelo proposto representa consistentemente as relações entre produtividade de arroz de sequeiro e déficit hídrico durante todo o ciclo da cultura em todas as regiões brasileiras, com menor dispersão na região Sul do que nas regiões Norte e Nordeste do país.

Bergamaschi et al. (2013) analisaram viabilidade de se estimar a produção de milho numa região subtropical do Sul do Brasil por meio do "general largeareamodel" (Glam) e observaram que modelos de grande escala podem contribuir para monitorar ou predizer padrões de variabilidade na produção de milho na região, estando altamente correlacionados com as produtividades observadas em grandes áreas.

Mabilana et al. (2012) na tentativa de ajustar um modelo agrometeorológico espectral para a estimativa de produtividade do milho na província de Manica em Moçambique, constataram que as variáveis agrometeorológicas e espectrais apresentam relação direta com a produtividade média de milho e que as expressões de modelos gerados evidenciam a potencialidade tanto do termo agrometeorológico, quanto do termo espectral na explicação das variações das produtividades médias de milho.

Santos e Camargo (2006) visando considerar os efeitos da produtividade do ano anterior e de temperatura adversas, modificaram e parametrizaram um modelo matemático agrometeorológico de monitoramento e de estimativa da quebra de produtividade do cafeeiro em diferentes regiões do estado de São Paulo. No referido trabalho concluíram que o modelo apresentou desempenho consistente na estimativa de produtividade para diferentes regiões.

Satapathy et al. (2014) avaliando o modelo CERES-arroz para previsão de produtividade em Kharagpur, Índia, observaram variação na produtividade da cultura em resposta à elevado dióxido de carbono em diferentes níveis de temperatura em cenários de mudanças climáticas.

Oliveira et al. (2012) ao avaliarem o modelo CROPGRO-Drybean como ferramenta de previsão de produtividade de feijão (*Phaseolusvulgaris* L.) cultivados em Viçosa, Minas Gerais, verificaram que o modelo se mostrou viável como ferramenta para a previsão da produtividade, obtendo estimativa adequada de produtividade com 30 dias de antecedência da colheita.

Modelos agrometeorológicos que fazem previsões de produtividade para espécies de palmeiras são menos usuais na literatura científica. Entretanto, podem-se mencionar os estudos conduzidos por Keong e Keng (2012) que tentaram desenvolver modelo agrometeorológico para previsão de produtividade mensal para a cultura da Palma de óleo (*Elaeis guineensis*), por meio de modelo de regressão linear múltipla. Nesse trabalho verificaram que é possível prever uma produtividade de óleo para essa espécie por nove meses com boa precisão, indicando que 68% da variabilidade da produtividade mensal foi bem representadas pelo modelo de regressão. No caso das espécies do gênero *Euterpe*, mais precisamente para o açaizeiro (*E. oleracea* Mart.), são inexistentes trabalhos na literatura com aplicação dos modelos de previsão ou estimação, apesar de apresentar expressivo valor de comercialização dentro e fora do Brasil.

Na literatura disponível há diversos modelos agrometeorológicos que usam regressões lineares simples ou múltiplas para estimativas ou previsões de produtividade de outras culturas anuais e perenes. A maior dificuldade nesta técnica está em selecionar quais variáveis independentes trazem mais informações e melhores resultados para os modelos (MORETO e ROLIM, 2015). A exemplo do trabalho de Junes e Fontana (2011), que desenvolveram uma regressão linear múltipla, construída a partir de indicadores agrometeorológicos (precipitação pluvial, índice de geadas e graus-dia) e espectrais (NDVI) para obterem a estimativa da produtividade de trigo no norte do Rio Grande do Sul, caracterizando de forma adequada as condições ambientais e seus efeitos na definição da produtividade final de lavouras de trigo.

Fahlel et al. (2005) desenvolveram uma metodologia para estimar a produtividade no cafeeiro, utilizando as características fenológicas determinantes do crescimento e produção em duas épocas de avaliação, onde encontrou resultados com precisão superior a 93%, permitindo a previsão de safras com até 6 meses de antecedência.

Assad et al. (2007) utilizaram os princípios de Doorenbos e Kassam (1979) para previsão da produtividade em soja, avaliando a perda da produtividade da cultura com o déficit hídrico, e encontraram bons resultados com (r^2 = 0,87), incorporando ajustes empíricos para cada região do Brasil e considerando diferenças quanto ao potencial produtivo das principais variedades.

Santos et al. (2011) também aplicaram o modelo proposto por Doorenbos e Kassam (1979) na mesorregiões de Minas Gerais para avaliar a relação seca/produtividade agrícola, em cenário de mudanças climáticas na cultura do milho, e constataram que se as cultivares, as práticas de manejo e as tecnologias atuais fossem mantidas e, caso as condições futuras do clima tendessem ao cenário de emissões A1B, a mudança projetada do clima teria um efeito negativo na produtividade de milho para o local avaliado.

Segundo Frizzone et al. (2005) as principais relevâncias quanto aos modelos agrometeorológicos, relacionam-se às suas aplicações, consideradas muitas vezes específicas para uma região ou incompletas no sentido de omitir efeitos de outros fatores e suas interações com a água. Entretanto, modelos regionalizados podem trazer uma acurácia maior em suas previsões como demonstrado por Moreto e Rolim (2015) quando comparados com modelos mais generalistas e que podem ser desenvolvidos a partir de dados meteorológicos provenientes de modelos globais, como o ECMWF.

1.1.2 Modelo ECMWF

O ECMWF (European Center for Medium-Range Weather Forecast) possui dados meteorológicos provenientes de modelos globais, muitos utilizados nas previsões de tempo e clima no mundo. Este Centro disponibiliza dados em uma amostragem (grid) de 0,25° (aproximadamente 25x25km) para todo o globo terrestre, tornando-se assim interessante para obtenção informações em regiões com escassez de estações meteorológicas de superfície (MORAES et al., 2012).

Jung et al. (2012) demonstraram que as integrações de clima com o ECMWF utilizando as resoluções horizontais, normalmente usados em previsões numéricas de tempo, levam a melhorias moderadas quando comparadas com a baixa resolução, pelo menos em aspectos de macroescala.

Na Amazônia a aplicação de modelos do ECMWF vem sendo realizadas, objetivando identificar as características atmosféricas de macro e meso escalas que expliquem os padrões climáticos da região (CAVALCANTI et al., 2016; COUTINHO et al., 2016; MARENGO, 2005).

Outros trabalhos como os de Person e Grazziani (2007) e Deppe et al. (2007) identificaram subestimação ou superestimação do modelo ECMWF em comparação as estações meteorológicas de superfície. Dessa forma, se faz importante uma avaliação prévia para uso dos dados do ECMWF como representativos das condições meteorológicas da região que se deseja trabalhar., como a do estado do Pará para a orientação da cultura do açaizeiro. Uma vez que não há registros

1.1.3 Cultura do Açaizeiro

O açaizeiro (*Euterpe oleracea* Mart) é uma palmeira de hábito perene possuindo frutos bastante valorizados para o preparo de bebidas. Pertence à família Arecaceae, que engloba aproximadamente 200 gêneros e cerca de 2600 espécies, cuja distribuição é predominantemente tropical e subtropical (GOLDEL et al., 2015). Na Amazônia está família encontra-se representada por 39 gêneros e por um número variável de espécies, entre 150 a 180 (KAHN, 1997). Nessa região o açaizeiro desempenha importante papel socioeconômico e ambiental nas áreas produtoras (VALLEJO et al., 2014), com aumentos nos retornos sociais do cultivo, após a inserção tecnológica na produção na ordem de 238 milhões de reais no ano de 2005, por meio de linhas de crédito de financiamento feitas pelos bancos (SILVA et al., 2006).

O novo contexto de mercado do açaí, tanto em nível nacional como internacional, tem se caracterizado por uma demanda crescente e superior à oferta, o que vem pressionando o aumento dos preços da polpa processada, sobretudo com o aumento das demandas de exportação (HOMMA e SANTANA, 2009). Nesses mercados a bebida é comercializada como commodity, onde o fator determinante é o preço, que oscila devido a sazonalidade da safra que se concentra no Pará, Amapá e Maranhão (NOGUEIRA et al., 2005).

No Brasil, o cultivo do açaizeiro vem ocorrendo em vários estados, mas com alta concentração nos estados da região norte, especialmente no Pará. A espécie ocorre espontaneamente, no Amapá, Maranhão, Pará (CALZAVARA 1972; CAVALCANTE, 1991), Tocantins (BALICK, 1986) e no Mato Grosso (Macedo, 1995). Fora do Brasil o açaizeiro é encontrado na Guiana Francesa, Suriname, Venezuela (CALZAVARA 1972; ROOSMALEN, 1985; CAVALCANTE, 1991) e Colômbia (BALICK, 1986). No entanto, as maiores áreas ocupadas com essa espécie, encontram-se na Amazônia oriental brasileira, mas precisamente na região do estuário do rio Amazonas, considerada como seu centro de origem.

Martorano et al. (1992) ressaltam que nessa região se concentra a maior produção nacional de açaí, estando inserida na zona equatorial, que é marcada por duas estações do ano, uma de maior e outra de menor oferta pluvial. Segundo esses autores, essa região está associada a fenômenos de grande e meso escala alterando as safras anuais de cultivo e a comercialização nos principais mercados consumidores como São Paulo e Rio de Janeiro e o mercado internacional.

Em estatísticas nacionais o Pará lidera a produção de açaí, com 60% da produção (IBGE, 2013) sendo o principal produto agrícola do estado com potencial para crescer ainda mais, acompanhando o aumento do interesse por parte de consumidores nacionais e internacionais. Da produção total, mais de 90% é originária de açaizais nativos das regiões de várzea. Entretanto, as regiões de terra firme também começam a despontar como regiões produtoras, com a incorporação de técnicas de reposição hídrica.

Na região Amazônica o açaizeiro floresce e frutifica durante todo o ano, mas, com picos nos meses de janeiro a maio e de setembro a dezembro, respectivamente (OLIVEIRA et al, 2002). O período de floração mais intensa coincide com a época de maior precipitação, enquanto o de frutificação predomina na época mais seca do ano (CALZAVARA, 1972; OLIVEIRA e FERNANDES, 1993). O aparecimento do ramo florífero está diretamente relacionado com a queda da folha, sendo que um dos principais fatores para que todo ramo complete seu ciclo, com a emissão da inflorescência e, posteriormente, do cacho, tem-se a disponibilidade hídrica do local (OLIVEIRA et al., 2000).

Em cultivos dessa espécie de açaizeiro em Ubatuba, litoral de São Paulo, foi verificado dois picos de florescimento, o primeiro nos meses de abril e junho e o segundo no período de outubro a dezembro, com a produção de frutos praticamente durante o ano todo (BOVI et al., 1986). Nesse local o açaizeiro vem sendo cultivado experimentalmente, visando à produção de palmito, estando sujeito à temperatura média anual mais baixa, em torno de 21°C, considerada por Aguiar (1988) como, provavelmente, próxima do limite mínimo de exigência térmica para a cultura.

Conforto et al. (2009) em estudos objetivando investigar o comportamento das variáveis biométricas e das trocas gasosas em plantas jovens de açaizeiro Cv. BRS Pará na fase de viveiro, quando submetidas a dois níveis de atenuação da radiação em condições ideais de fornecimento hídrico, observaram potencial para a produção de mudas em Ribeirão Preto, SP, sobretudo se forem mantidas sob atenuação de 50% de irradiância.

Calbo e Moraes (2000) avaliando plantas de *Euterpe oleracea* de quatro meses de idade em São Carlos (SP) identificaram mecanismos de adaptação a estresse hídrico moderado, tornando-se um fator promissor para o cultivo do açaizeiro no interior do Estado. Essas particularidades permite a expansão do cultivo do açaizeiro em regiões não tradicionais do Brasil, no entanto, apresenta uma produção que ainda demanda de pesquisas que visem o melhor manejo do cultivo, assim como o conhecimento de áreas com potencial climático para sua expansão.

1.1.4 Referências

AGUIAR, C.J.S. Contribuição para a implantação da cultura do açaizeiro (*Euterpe oleracea* Mart.) no litoral paulista. In: **Encontro nacional de pesquisadores em palmito**. Anais. Curitiba: Embrapa-CNPF, p. 75-90 (Embrapa-CNPF. Documentos, 19). 1988.

ASSAD, E.D.; MARIN, F.R.; EVANGELISTA, S.R.; PILAU, F.G.; FARIAS, J.R.B.; PINTO, H.S.; JULLO JÚNIOR, J. Sistema de previsão da safra de soja para o Brasil. **Pesquisa Agropecuária Brasileira**, v.42, p.615-625, 2007.

BALICK, M.J. Palms and development in the humid tropics. Belém: **Embrapa-CPATU**, v, 6, p.121- 140,1986. (Embrapa-CPATU. Documentos, 36).

BECHTOLD, P.; KOHLER, M.; JUNG, T.; DOBLAS-REYES, F.; LEUTBECHER, M.; RODWELL, M.J.; VITART, F.; BALSAMO, G. Advances in simulating atmospheric variability with the ECMWF model: From synoptic to decadal time-scales. **Q. J. R. Meteorol. Soc**. v. 134, p. 1337 – 1351, 2008.

BERGAMASCHI, H.; COSTA, S. M. S.; WHEELER, T.R.; CHALLINOR, A.J. Simulating maize yield in sub-tropical conditions of southern Brazil using Glam model. **Pesq. agropec. bras.**, Brasília, v.48, n.2, p.132-140, 2013.

BOVI, M.L.A; DIAS, G. S; GODOY JÚNIOR, G. Biologia floral do açaizeiro (*Euterpe oleracea* Mart.). In: **CONGRESSO DA SOCIEDADE DE BOTÂNICA DE SÃO PAULO**. São Paulo. Resumos. UNICAMPI, p.91, 1986.

CALBO, M.E.R.; MORAES, J. A. P.V. Efeitos da deficiência de água em plantas de *Euterpe oleracea* (açaí). **Revista brasil. Bot.**, São Paulo, v.23, n.3, p.225-230, 2000.

CALZAVARA, B.B.G. As possibilidades do açaizeiro no estuário amazônico. Belém: FCAP. **Boletim da Faculdade de Ciências Agrárias do Pará**, p. 5-103, 1972. (Embrapa- CPATU. Documentos, 36).

CAVALCANTE, P. **Frutas comestíveis da Amazônia**. Belém: CEJUP, 271p, 1991.

CAVALCANTI, I. F. A.; MARENGO, J. A.; ALVES, L. M.; COSTA, D. F. On the opposite relation between extreme precipitation over west Amazon and southeastern Brazil: observations and model simulations. **Int. J. Climatol.** 2016.

CESS, R. D.; POTTER, G. L.; BLANCHET, J. P.; BOER, G. J.; GHAN, S. J.; KIEHL, J.T.; LE, TREUT H.; LI, ZX.; LIANG, XZ.; MITCHELL, J. F.; MORCRETTE, J. J.; RANDALL, D. A.; RICHES, M. R.; ROECKNER, E.; SCHLESE, U.; SLINGO, A.; TAYLOR, K.E.; WASHINGTON, W.M.;

WETHERALD, R. T.; YAGAI, I. Interpretation of cloud-climate feedback as produced by atmospheric general circulation models. **Science**. 1989.

CONFORTO, E.C.; CONTIN, D. R. Desenvolvimento do açaizeiro de terra firme, cultivar Pará, Sob atenuação da radiação solar em fase de viveiro. **Bragantia.** v.68, n.4, p.979-983, 2009.

COUTINHO, M. D. L.; LIMA, K. C.; SILVA, C. M. S. Regional climate simulations of the changes in the components of the moisture budget over South America. **Int. J. Climatol**. v. 36, p. 1170–1183, 2016.

DEPPE, F.; MARTINI, L.; LONHMANN, M.; CALVETTI, L.; ADAMI, M. Comparação de estimativas de precipitação com dados observados (estações meteorológicas). In: XII **SIMPÓSIO BRASILEIRO DE SENSORIAMENTO REMOTO (SBSR)**. Florianópolis/SC. Anais... São José dos Campos: INPE, p.3319-3326, 2007.

FAHL, J.I.; CARELLE, M.L.C.; ALFONSI, E.L.; CAMARGO, M.B.P. Desenvolvimento e aplicação de metodologia para estimativa de produtividade do cafeeiro, utilizando as características fenológicas determinantes do crescimento e produção em duas épocas de avaliação. In: **Congresso Brasileiro de Pesquisa Cafeeira**. Guarapari. Anais. Guarapari: MAPA/PROCAFÉ. p.339-341.2005.

FRIZZONE, J. A.; ANDRADE JÚNIOR, A. S.; SOUZA, J. L. M.; ZOCOLER, J. L. **Funções de produção água-cultura. In: Planejamento de irrigação: análise e decisão de investimento**. Brasília: Embrapa, p. 283-314. 2005.

GATES, W.L.; BOYLE, J.; COVEY, C.; DEASE, C.; DOUTRIAUX, C.; DRACH, R.; FIORINO, M.; GLECKLER, P.; HNILO, J.; MARLAIS, S.; PHILLIPS, T.; POTTER, G.; SANTER, B.D.; SPERBER, K.R.; TAYLOR, K.; WILLIAMS, D. An Overview of the Results of the Atmospheric Model Intercomparison Project (AMIP I). Bull. **Am. Met. Soc**. v.80, p. 29-55. 1999.

GÖLDEL, B.; KISSLING, W.D.; SVENNING, J.C. Geographical variation and environmental correlates of functional trait distributions in palms (Arecaceae) across the New World. **Botanical Journal of the Linnean Society**, v. 179, p. 602–617, 2015.

HOMMA, A.K.O.; SANTANA A.C. **A agroindústria na Região Norte**, In: Zibetti DW & Barroso LA (Eds.) Agroindústria: uma análise no contexto socioeconômico e jurídico brasileiro. LEUD São Paulo, v.1, p.19-43. 2009.

IBGE - **Instituto Brasileiro de Geografia e Estatística**. Levantamento sistemático da produção agrícola: 2013. Disponível em: <www.ibge.gov.br/home/estatistica/indicadores/ agropecuaria/lspa/>. Data de acesso: 02/09/2015.

JUNES, A. H.; FONTANA, D. C. Modelo agrometeorológico-espectral de estimativa de rendimento de grãos de trigo no Rio Grande do Sul. **Rev. Ceres**, v. 58, n.1, p. 9-16, 2011.

KAHN, F. Les palmiers de l"eldorado. Paris: Éditions de l"Oprstom. **Journal of Nutrology**. p. 252. 1997.

KEONG, Y. K.; KENG, W. M. **Statistical Modeling of Weather-based Yield Forecasting for Young Mature Oil Palm**. ICAAA. 2012. Faltou o número de páginas.

LAMBERT, S. J.; BOER, G. J. CMIP1 evaluation and intercomparison of coupled climate models, **Clim. Dyn**. v. 17, p. 83–106. 2001.

MABILANA, H. A.; FONTANA, D. C.; FONSECA, E. L. Desenvolvimento de modelo agrometeorológico espectral para estimativa de rendimento do milho na Província de Manica-Moçambique. **Rev. Ceres**, v. 59, n.3, p. 337-349, 2012.

MACEDO, M. Contribuição ao estudo de plantas econômicas no Estado de Mato Grosso. Cuiabá: **UFMT**, 70p. 1995.

MARENGO, J. A. Characteristics and spatio-temporal variability of the Amazon River Basin Water Budget. **Climate Dynamics**, v. 24, p. 11–22. 2005.

MARTORANO, L.G.; PERREIRA, L.C.; CÉSAR, E.G.M.; PEREIRA, I.C.B. Estudos Climáticos do Estado do Pará, Classificação Climática (KÓPPEN) e Deficiência Hídrica (Thornthwhite&Mather). **Belém, SUDAM/ EMBRAPA, SNLCS**. 53p.1992.

MIRIN, A. A.; SAWYER, W.B. A scalable implementation of a finite-volume dynamical core in the community atmosphere model. **Int. J. High Perform. Comput. Appl**. v.19, p. 203–212, 2015.

MONTEIRO, J. E. B. A.; AZEVEDO, L. C.; ASSAD, E. D.; SENTELHAS, P. C. Rice yield estimation based on weather conditions and on technological level of production systems in Brazil. **Pesq. agropec. bras**. v.48, n.2, p.123-131, 2013.

MORAES, R. A.; ROCHA, A. V.; ROLIM, G. S.; LAMPARELLI, R. A.C.; MARTINS; M. M. Avaliação dos dados decendiais de precipitação e temperatura máxima e mínima do ar simulados pelo modelo ECMWF para o estado de São Paulo. **Irriga**. v.17, n,3, p. 397-407, 2012.

MORETO, V. B.; ROLIM, G. S. Estimation of annual yield and quality of Valência orange related to monthly water deficiencies. **African Journal of Agricultural Research**, v. 10, p. 543-553, 2015.

NAKAEGAWA, T.; KITOH, A.; ISHIZAKI, Y. Caribbean low-level jets and accompanying moisture fluxes in a global warming climate projected with

CMIP3 multi-model ensemble and fine-mesh atmospheric general circulation models. **Int. J. Climatol**. v.34, n. 4, p. 964–977, 2014.

NASCIMENTO, C.N.B.; HOMMA, A.K.O. Amazônia: meio ambiente e tecnologia agrícola. Belém: **Embrapa-CPATU**. 282p. 1984. (Embrapa-CPATU. Documentos, 27).

NOGUEIRA, O.L.; FIGUEIRÊDO, F.J.C.; MULLER A.A. Açaí. Embrapa Amazônia Oriental. Belém, Pará. **(Sistemas de Produção, 4)**. p.137, 2005.

OLIVEIRA, E. C.; COSTA, J. M. N.; PAULA JÚNIOR, T. J.; FERREIRA, W. P. M.; JUSTINO, F. B.; NEVES, L. O. The performance of the CROPGRO model for bean (*Phaseolus vulgaris* L.) yield simulation. **Acta Scientiarium**, v.34, p.239-246, 2012.

OLIVEIRA, M.S.P. Biologia floral do açaizeiro em Belém, PA. Embrapa Amazônia Oriental. **Boletim de Pesquisa e Desenvolvimento**, 26p, 2002.

OLIVEIRA, M.S.P.; CARVALHO, J.E.U.; NASCIMENTO, W.M.O. **Açaí (*Euterpe oleracea* Mart.)**. Jaboticabal: Funep, 52p. 2000. (Série Frutas Nativas, 7).

OLIVEIRA, M.S.P.; FERNANDES, T.S.D. Aspectos da floração do açaizeiro (*Euterpe oleracea* Mart.) nas condições de Belém-PA. In: **CONGRESSO NACIONAL DE BOTÂNICA**, 44, São Luís. Resumos. São Luís: SBB, 159p.1993.

PEREIRA, A.R.; ANGELOCCI, L.R.; SENTELHAS, P.C. **Agrometeorologia: fundamentos e aplicações práticas**. Guaíba: Agropecuária, 478p. 2002.

PERSON, A.; GRAZZIANI, F. User guide to ECMWF forecast products. **Meteorological Bulletin M3.2. Reading,UK: ECMWF,** 153p. 2007.

PICINI, A. G.; CAMARGO, M. B. P.; ORTOLANI, A.A.; FAZUOLI, L.C.; GALLO, P.B. Desenvolvimento e teste de modelos Agrometeorológicos para estimativa de produtividade do cafeeiro. **Bragantia**, v.58, p.157-170, 1999.

REICHLER, T.; KIM, J. How Well do Coupled Models Simulate Today's Climate? Bull. **Amer. Meteor. Soc**. v.89, p. 303-311, 2008.

ROLIM, G. S.; RIBEIRO, R. V.; AZEVEDO, F. A.; CAMARGO, M. B. P.; MACHADO, E. C. Previsão do número de frutos a partir da quantidade de estruturas reprodutivas em laranjeiras. **Revista Brasileira de Fruticultura**, v. 30, p. 48-53, 2008.

ROOSMALEN, M.G.M. **Fruits of the Guianan Flora**. Utrecht: Institute of SystematicsBotany/Wageningen Agricultural University, 483p. 1985.

SANTOS, M. A.; CAMARGO, M. B. P. Parametrização de modelo agrometeorológico de estimativa de produtividade do cafeeiro nas condições do Estado de São Paulo. **Bragantia**, v.65, n.1, p.173-183, 2006.

SANTOS, R. S. S.; COSTA, L. C.; SEDIYAMA, G. C.; LEAL, B. G.; OLIVEIRA, R. A.; JUSTINO, F. B. Avaliação da relação seca/produtividade agrícola em cenário de mudanças climáticas. **Revista Brasileira de Meteorologia**, v.26, n.2, p. 313 - 321, 2011.

SATAPATHY, S.S.; SWAIN, D.K.; HERATH, S. Field experiments and simulation to evaluate rice cultivar adaptation to elevated carbon dioxide and temperature in sub-tropical India. **Eur. J. Agron**. v. 54, p. 21–33. 2014.

SATOH, M. Standard experiments of atmospheric general circulation models, in: Atmospheric Circulation Dynamics and General Circulation Models. **Springer, Berlin, Heidelberg**. p. 689–702. 2014.

SILVA, I. M.; SANTANA, A. C.; REIS, M. S. Análise dos retornos sociais oriundos de adoção tecnológica na cultura do açaí no Estado do Pará. Amazônia: **Ciência & Desenvolvimento**, v. 2, p. 25-37, 2006.

VALLEJO, M. I.; GALEANO G.; BERNAL R.; ZUIDEM, P.A. The fate of populations of *Euterpe oleracea* harvested for palm heart in Colombia. **Forest Ecology and Management**. v. 318, p. 274–284, 2014.

WANG, H., L. LONG, A. KUMAR, W. WANG, J.-K.E. SCHEMM, M. ZHAO, G.A. VECCHI, T.E. LAROW, Y.-K. LIM, S.D. SCHUBERT, D.A. SHAEVITZ, S.J. CAMARGO, N. HENDERSON, D.Y. KIM, J.A. JONAS, and K.J.E. Walsh, 2014: How well do global climate models simulate the variability of Atlantic tropical cyclones associated with ENSO.?. **J. Climate**, 27, no. 15, 5673-5692.

WANG, Y; JIANG, J; ZHANG H; DONG, X.; WANG, L.; RANJAN, R; ZOMAYAF, A. Y. A scalable parallel algorithm for atmospheric general circulation models on a multi-core cluster. **Future Generation Computer Systems.** v. 72, p.1–10, 2017.

CAPÍTULO 2 - PERFORMANCE OF THE ECMWF MODEL IN AIR TEMPERATURE AND PRECIPITATION ESTIMATES IN THE BRAZILIAN AMAZON

Abstract

We evaluated the performance of general atmosphere circulation model (GCM) from the European Center for Medium Range Weather Forecasts (ECMWF) for estimating surface air temperature (T) and precipitation (P) in 55 locations in the Brazilian Amazon for10-day period and monthly period. We compared data from surface meteorological stations obtained by the Brazilian Institute of Meteorology (INMET) and ECMWF by linear regression analysis (LRA) using R^2 and Willmott (1985) index (d) as measurement of precision and accuracy, respectively. In order to represent the P regime in the Brazilian Amazon we applied the Fourier series analysis by extracting the trend and frequency components of the rainfall events (P) with noise reduction in the time series. We used the multivariate K-means method to separate weather stations by Groups of Similar Performances (GSPs). A stratification was performed in two characteristic periods of the region, the dry (August to October, P< 125 mm month^{-1}) and rainy (February to April, P > 250 mm month^{-1}) seasons. The northwest region is characterized as the area with the highest rainfall supply but the lowest performances for T and P, with R^2 lower than 0.18. ECMWF tend to overestimate P in dry season and to underestimate it in rainy season. The proposed methodology of calibration of P data by the Fourier series was a good tool to predict an extreme event every 5 to 7 months in the region. The ECMWF model presented high performance (R^2> 0.60) when estimating P in monthly scale and medium performance (R^2<0.60) when estimating Tin monthly and10-day period. The highest concentrations of surface meteorological stations in the eastern/southeastern portion of the Amazon region were decisive in the ECMWF performance expression, indicating an increased meteorological predictability in the anthropic areas, precisely where the agricultural areas of grain were established in the region.

Keywords: amazon forest; fourier analysis; K-means; modeling; regression analysis

2.1 Introduction

Amazon has large spatio-temporal variations of rainfall (Marengo and Espinoza, 2016) and high annual temperatures (Taylor et al., 2017), which shows the importance of the predictability of weather and climate conditions to support agrometeorological planning in agricultural crops. With a total area of 5 217423 km^2, the Brazilian Amazon accounts for 61% of the Brazilian territory (Martha et al., 2011) which corresponds roughly to the area of European Russia, France and Spain together. It presents a wide variety of ecosystems, and it is the largest tropical forest on the planet (Cheng et al., 2013; Drumond et al., 2014).

The Amazon region contributes to almost 18% of the total discharge of fresh water into the Atlantic Ocean (Marengo and Nobre, 2009; Callèdeet al., 2010). The variation of its water balance and energy greatly affects the transport of atmospheric humidity, whih plays an important role in global and regional climate, contributing to atmospheric circulation in the tropics (Werth and Avissar, 2002; Cox et al., 2008). However, sea surface temperature variations in the Pacific and Atlantic oceans modulate the regional rainfall and hydrological variability (Marengo and Espinoza, 2016).

Because of the importance of the Amazon basin in a global, regional and local scales, studies of thermo-pluviometric conditions are necessary for a more complete understanding of the climate variability and changes (Lee and Ouarda, 2010; Yang et al., 2010; Sang et al., 2012). However, the density of meteorological stations on the surface of that region is still low (Drumond et al., 2014) with approximately one station for each 90,000 km^2, which restricts the evaluation of predictability of weather and climate conditions in the region.

There is a lack of comprehensive information capable of structuring robust databases to model processes, as well as testing the performance of numerical models to estimate response variables such as energy and water balance (Marengo, 2005). General circulation models (GCM) is an option for this meteorological monitoring and forecasting. These models join surface information, airplanes and buoys in the oceans and satellites from all over the planet to make gridded estimations and forecastings. These kind of systems include the European Center for Medium Range Weather Forecasts (ECMWF) which estimates climate data and has been applied in several areas such as industry, tourism, insurance and agriculture.

The ECMWF system contributes substantially to the supply of data in regions with few surface meteorological stations (Alessandrini et al., 2013; Ceglar et al., 2016). The ECMWF has been used in the Amazonian region with several purposes, such as to identify the atmospheric characteristics in macro and meso scales that explain the climatic patterns of the region (Cavalcanti et al., 2016; Coutinho et al., 2016; Ring et al., 2016). However, there is a lack of validation of ECMWF in comparison to real time series data from surface stations.

In some studies, statistical methods have been applied to investigate the periodic component of time series, which can be analyzed by three indices: period, trend and noise (Elshorbagyet al., 2002; Clara et al., 2014; Sawaske and Freyberg, 2014, Tanaka et al., 2015).

Among the methods, Fourier analysis (FFT), suitable for the treatment of stationary data (Sypkaet al, 2016), has the advantage of providing a high perception in the processes that control the climatic phenomena. In addition, the physical consistency of such estimates allows the recognition of potential spurious samples in the baseline data, which could not be detected by other statistical methods (Laguardia, 2011).

In assessing the effectiveness of the Fourier series to represent the climate and environmental variables regime, Laguardia (2011) applied precipitation data in Italy and verified that the estimated and interpolated rains described the pluvial regime in a more compact and consistent way, reducing the complexity of the spatial variation of the rain regime.

We evaluated the performance of the General Atmospheric Circulation Model (GCM) from the European Center for Medium Range Weather Forecasts (ECMWF) for estimating surface air temperature (T) and precipitation for 55 locations in the Brazilian Amazon for a 10-day and monthly periods.

2.2 Material and methods

Daily data of mean air temperature (T) and rainfall (P) of 55 surface meteorological stations were obtained from the National Institute of Meteorology (INMET) database, corresponding to the area of the Brazilian Amazon (Figure 1).Gridded data of 27 x 27 km from the ECMWF system were used for a 10-day period and are available at http://spirits.jrc.ec.europa.eu/. The ENVI software was used to extract the values of T and P corresponding to the locations of INMET surface stations.

T and P from 1990 to 2014 were organized 10-day and monthly periods for comparison between surface and ECMWF system.

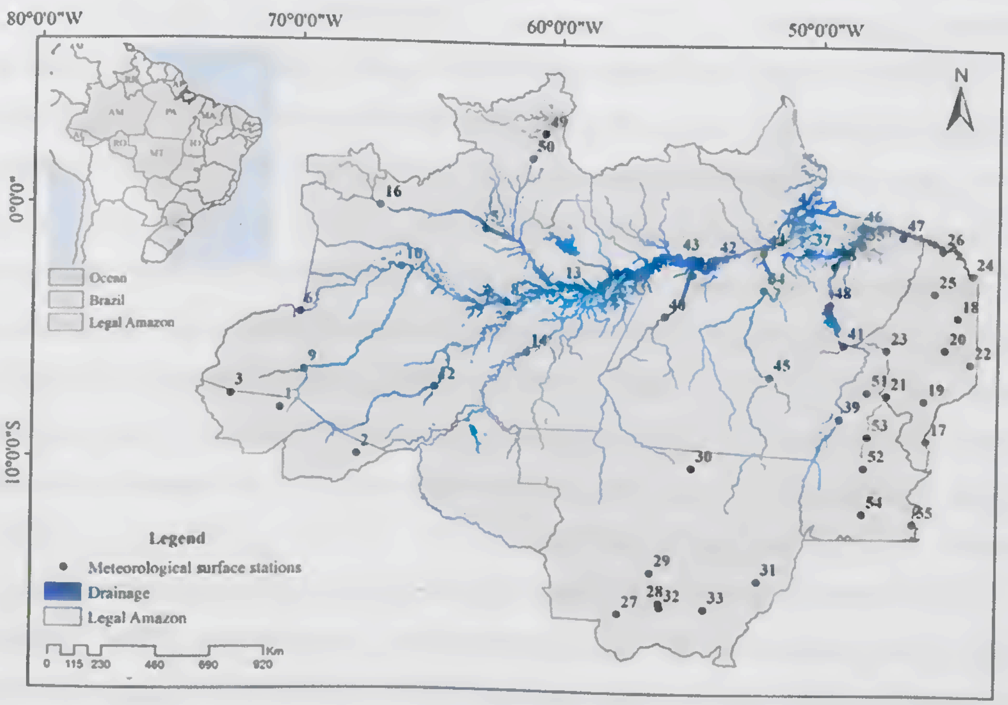

Figure 1. Surface weather station network from National Institute of Meteorology(INMET) in the Brazilian Amazon.

State of Acre (AC), 1-Tarauaca, 2-Rio Branco, 3-Cruzeiro do Sul. Amapá (AP), 4-Macapa. State of Amazonas (AM), 5-Barcelos, 6-Benjamin Constant, 7-Coari, 8-Codajas, 9-Eirunepe, 10-Fonte Boa, 11-Itacoatiara, 12-Labre, 13-Manaus, 14-Manicore, 15-Parintins, 16- São Gabriel da Cachoeira. State of Maranhão (MA), 17- Alto Parnaíba, 18-Bacabal, 19-Balsas, 20-Barra do Corda, 21-Carolina, 22-Colinas, 23-Imperatriz, 24- São luís, 25-Zé Doca, 26-Turiacu. State of Mato Grosso (MT), 27-Caceres, 28-Cuiaba, 29-Diamantino, 30-Matupa, 31-Nova Xavantina, 32-Padre Ricardo Remeter, 33-Poxoreo. State of Pará (PA), 34- Altamira, 35-Belém, 36-Belterra, 37-Breves, 38-Cametá, 39-Conceição do Araguaia, 40-Itaituba, 41-Marabá, 42-Monte Alegre, 43-Obidos, 44-Porto de Moz, 45-São Felix do Xingu, 46-Soure, 47-Tracuateua, 48-Tucurui.

State of Roraima (RR), 49-Boa Vista, 50-Caracarai. Tocantins (TO), 51-Araguaina, 52- Palmas, 53-Pedro Afonso, 54-Peixe, 55-Taguatinga.

The stations located in the Brazilian Amazon are installed in areas with altitude below 200 meters, totalizing about 75% of the surface stations that provide weather and climate information in the region, being the lowest altitude in Belém-PA, which is 10 meters above sea level. The monitoring in areas above 200 meters occurs mostly in Mato Grosso and Tocantins, with the highest elevation in the municipality of Taguatinga-TO, which is 603 meters (Figure 2).

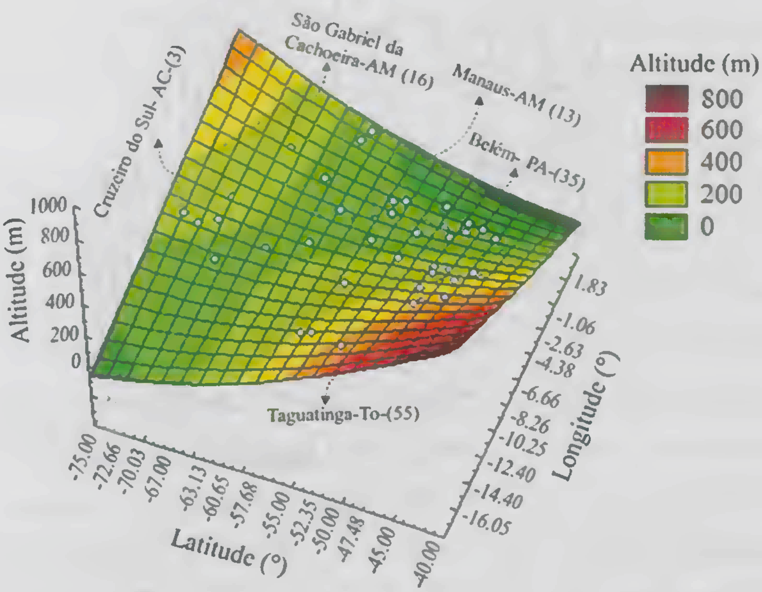

Figure 2. Altitude of meteorological stations in the Brazilian Amazon.

To evaluate the accuracy of T and P for a 10-day and monthly period estimated by the ECMWF we used the linear regression analysis (LRA) utilizing the surface data (INMET) as dependent variables and ECMWF data as independent variables. The statistics used to evaluate the performance of the adjustments were the precision by the coefficient of determination (R^2) and the accuracy by the coefficient of agreement of Willmott et al (1985) (d) (eq.1).

$$d = 1 - \frac{\sum_{i=1}^{N} (Yobs - Yest)^2}{\sum_{i=1}^{N} (|Yest - \overline{Yobs}|) + |Yobs - \overline{Yobs}|)^2} \quad (1)$$

where Yestis the estimated values; Yobsi is the observed values.

The outliers were identified by the HAT matrix test proposed by Hoaglin and Welsch (1978), resulting from the relationship between INMET and ECMWF sources. The identified outliers were removed from the analysis using the software developed by Moraes et al. (2017). The 55 sites were grouped regarding the precision (R^2) of each linear model adjusted.

R^2 were spatialized in the ArcGis software and grouped by the K-means multivariate method in 6 (six) group of similar performances (GSPs), according to the similarity of each variable (T and P) (Liu & Guo, 2016). Cluster analysis was used to identify the different homogeneous GSPs, according to their centroid (Jain et al., 1999).

The dynamics of T and P among the generated clusters were also analyzed by descriptive statistics, separating the data by dry (less rainy) and rainy season, typical thermal-water regime in the Brazilian Amazon. We used the values from August to October and from February to April, respectively, adopting the stratification by group of regions performed by Marengo (1992) and Delahaye et al. (2015) to characterize the climatic variability of the Amazon.

The temporal series of P have high variability in Amazon, with periodic components at various time intervals (Xie et al., 2016) to evaluate this variability. Thus, we apply the Fourier series (Eq. 2), aiming to quantify the trends and frequencies of each site studied. The variables generated by the Fourier series were also incorporated in the LRA, in an attempt to better estimate surface P monthly and 10-day periods from ECMWF data.

$$y(k) = \sum_{n=0}^{N-1} e^{-2\pi j \frac{kn}{n}} x(n) \quad \text{(Eq. 2)}$$

where N is the signal length(the number of samples in sequence); n and k are indices = 0. . .N-1; j is an imaginary unity ($\sqrt{-1}$).The Fourier functions are not limited to negative or positive functions, therefore, $e^{2\pi - j\frac{kn}{n}} = \cos\left(2\pi \frac{m}{N} n\right) + j\, sen\left(2\pi \frac{m}{N} n\right)$, and it is necessary to have stationary data to perform the analysis (Olitaet al., 2011).

In order to verify the stationarity of the data, we applied the Dickey-Fuller test (Dickey and Fuller, 1979), observing the stationary and temporal properties of the process according to the methodology of MacKinnon (2010). As the p-value calculated by the Dickey-Fuller test for station GSPs is lower than the significance level (α = 0.05), we can conclude that the data are stationary, allowing the use of Fourier analysis.

With the precision (R^2) of the models, it was possible to use such values to produce a 10-day period and monthly P and T maps, interpolating the values using the Inverse Distance Weighted Method (IDW), as suggested by Harman et al. (2016).

The GSPs obtained by the K-means analysis were spatialized, evaluating their distribution based on the interpolation of R^2 values. We constructed maps to represent the spatial distribution of surface T and P variables from the corrected ECMWF data for Brazilian Amazon.

2.3 Results and discussion

Surface air temperatures (INMET) (T_{SUR}) in the Brazilian Amazon were higher during the year when compared to ECMWF (T_{ECMWF}) data, ranging from 26.8 °C to 28.4 °C and 25 °C to 27.1 °C, respectively, on the monthly scale. The lowest and highest values of T_{SUR} and T_{ECMWF} were in July and October, and in March and September, respectively (Figure 3).

The T_{ECMWF} were conservative, since they had smaller annual thermal amplitudes. In the period of higher T_{SUR}, between September to October, and in the period of small T_{SUR}, between June and July, the T_{ECMWF} were lower than T_{SUR}. However, the greatest difference in monthly T was only 2.0 °C between the two types of thermal information analyzed (Figure 3).

Surface precipitation (P_{SUR}) had high variability when comparing the rainy with the dry season in Brazilian Amazon. In the rainy and dry period the P_{SUR}

ranged from 420 mm to 20 mm, respectively. The P_{ECMWF} variation was between 45 mm and 350 mm in these two analyzed periods, with an overestimation by the model when compared to the surface data (P_{SUR}), both for the lowest and the highest P. P_{SUR} and P_{ECMWF} from February to April and July to September had the higher and lower values, respectively (Figure 3).

With the HAT matrix test, only 1.98% of the T data and 2.53% of P were identified as outliers, indicating that ECMWF data were robust enough to estimate the surface data.

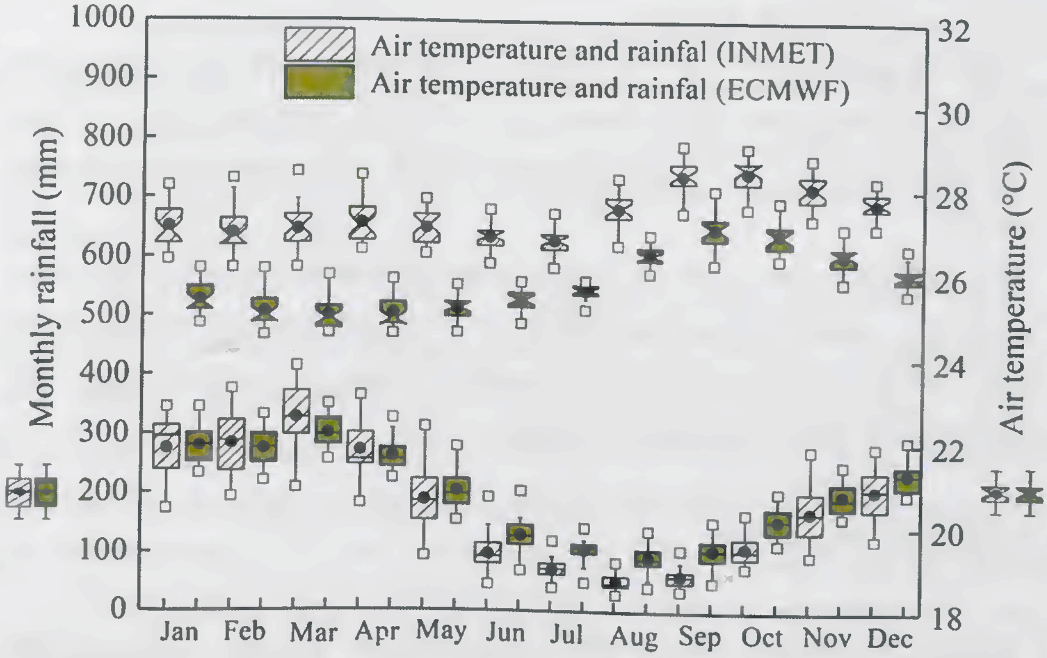

Figure 3. Box-plot of monthly data of air temperature and rainfall of INMET surface stations and ECMWF grid data in the Brazilian Amazon. Box plot is monthly rainfall (mm) and, notched box is air temperature (°C).

This characterization of the Amazonian climate regime was also pointed out by several authors (Marengo, 1992; Liebmann and Marengo, 2001; Espinoza et al., 2009a; Gloor et al., 2013; Delahaye et al., 2015; Marengo and Espinoza, 2016), who observed that the most rainy regions of the Amazon are located near the Atlantic Ocean, under the preponderant influence of the Zone of Intertropical Convergence (ITCZ) (Figure 4).

According to Doughty et al. (2012), the possible reasons for lower precipitation in these peripheral regions of Amazon are attributed to the recirculating water into the atmosphere, altering the annual dynamics of the ITCZ due to changes in the albedo, which is caused by the loss of surface cover as a consequence of deforestation or changes in water vapor exports from the Southeast basin (Espinoza et al., 2009b).

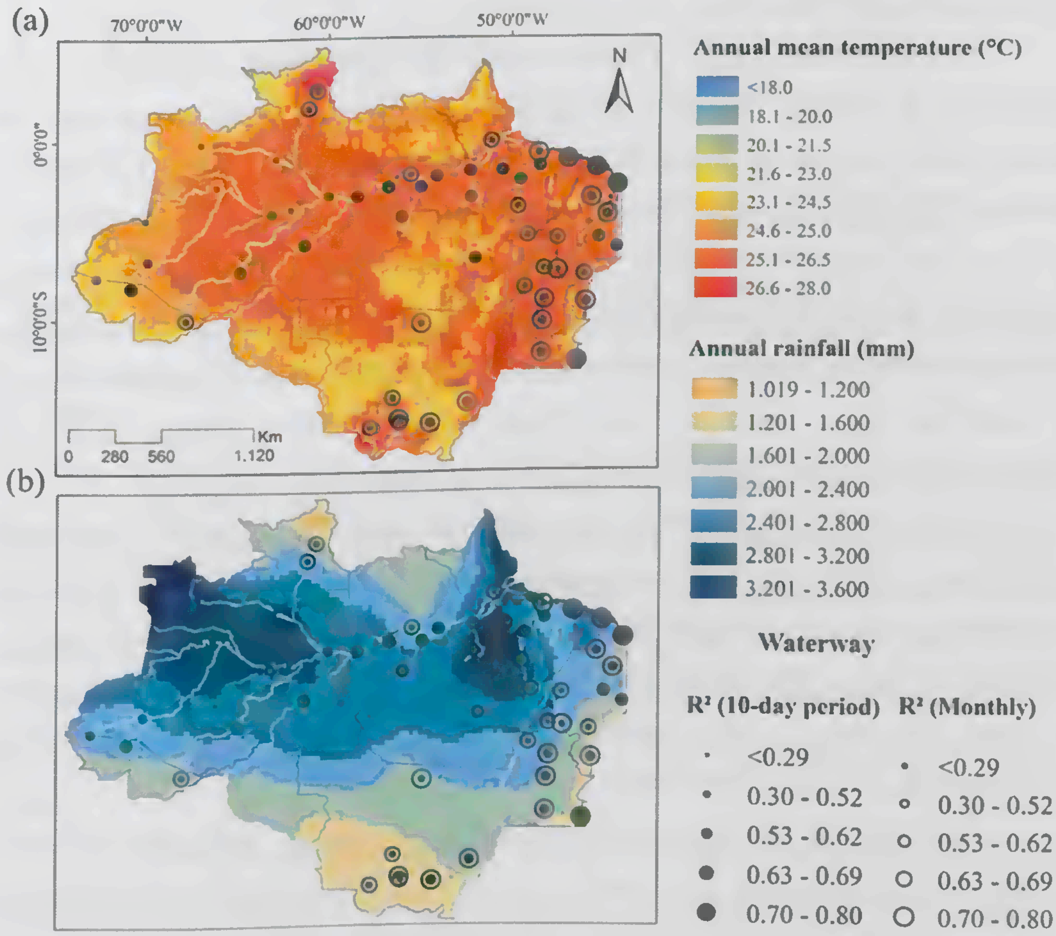

Figure 4. Spatialization of R^2 values in the Brazilian Amazon for surface air temperature (a) and precipitation (b) estimated by the ECMWF grid data.

The adjustments made to LRAs developed for all 10-day period and monthly scales with estimates of T_{SUR} and P_{SUR} ranged from (R^2) 0.29 to 0.80 in the localities (Figure 4). Therefore, there is a spatial dependence on the performance of the adjustments. The stations in the south, east and northeast of the Amazon had higher R^2 values in comparison to the northwest region. For example, the northwestern region has higher annual rainfall, resulting in an inverse proportionality ratio in R^2 accuracy (Figure 4(b)).

These results reinforce that the values estimated with greater precision occur in the northeast part of the Brazilian Amazon, precisely where it has a history of anthropization for more than 300 years, where in the last 20 years Oil Palm production has beenthe most important.

The low precision (R^2) of the models in some Brazilian Amazonian sites occurs due to the low coupling of ECMWF data to the surface because of several macro and meso scale factors. Among these factors, the convective systems in Amazon are quite complex and heterogeneous and are categorized as a special convective regime different from other regions in the world (Williams et al., 2002; Marengo 2005; Betts and Dias, 2010; Lin et al., 2016). The classical regimes present a more often organized convective systems, such as instability lines, however, the Amazon has a strong diurnal cycle of unorganized convective cells (Williams et al., 2002).

Betts and Jakobs (2002) demonstrated that the ECMWF prediction model has a known error in the daytime precipitation cycle on the Amazon, corroborating with Bechtold et al. (2004), who analyzed the ECMWF global prediction model on the southwest of the region. These observations reinforce that the convection in the Amazon occurs very early in the day cycle, demonstrating an error of estimation in ECMWF models.

In addition to the geographic position, R^2 values also had a direct connection to altitude and an inversely relation to continentality and annual P, both in 10-day period (5.AC, D) and monthly scales (Figure 5.D, E, F).

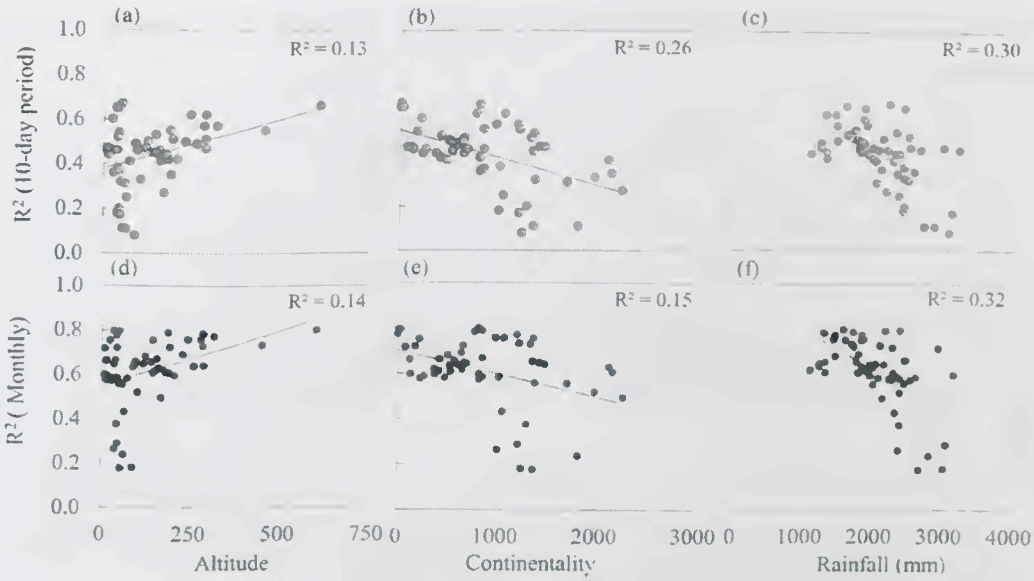

Figure 5. 10-day period and monthly analysis of continentality (a and d), altitude (b and e) and rainfall (c and f) respectively, in the Brazilian Amazon with the estimates of R^2 between the surface stations as a function of the ECMWF grid data.

We identified six GSPs of locations in the Brazilian Amazon when applying the K-means method, considering the 10-day period and monthly scales for T and P. It should be emphasized that this analysis allowed the selection of the models to be used in different regions of the Brazilian Amazon. For example, the highest distances of K-means for T occurred between GSPs 4 and 6 for 10-day period and GSPs 5 and 6 for monthly period (Figure 6(a) and 6(b)).

Euclidean distances determined by K-means analysis (Figure 6) for temperature and rainfall, monthly and for a10-day period, are directly related to R^2. For example, the GSP 6 for a 10-day period rain (Figure 6 (c)) and monthly rain (Figure 6 (d)) with the largest Euclidean distances (> 1) have R^2 of 0.63 (Figure 9 (f)) and 0.76 (figure 10 (f)), respectively. Conversely, also for rain, GSP 4 showed the lowest negative correlations and precision.

The precision (R^2) of GSPs were not dependent on the number of selected weather stations of the regions (Figure 4). For example, GSP 6 (Figure 6 (c)) there are 6 meteorological stations with R^2 of 0.63. However for GSP 2, there are 19 weather stations withR^2 of 0.42 (Figure 9 (f) and 9 (B), respectively).

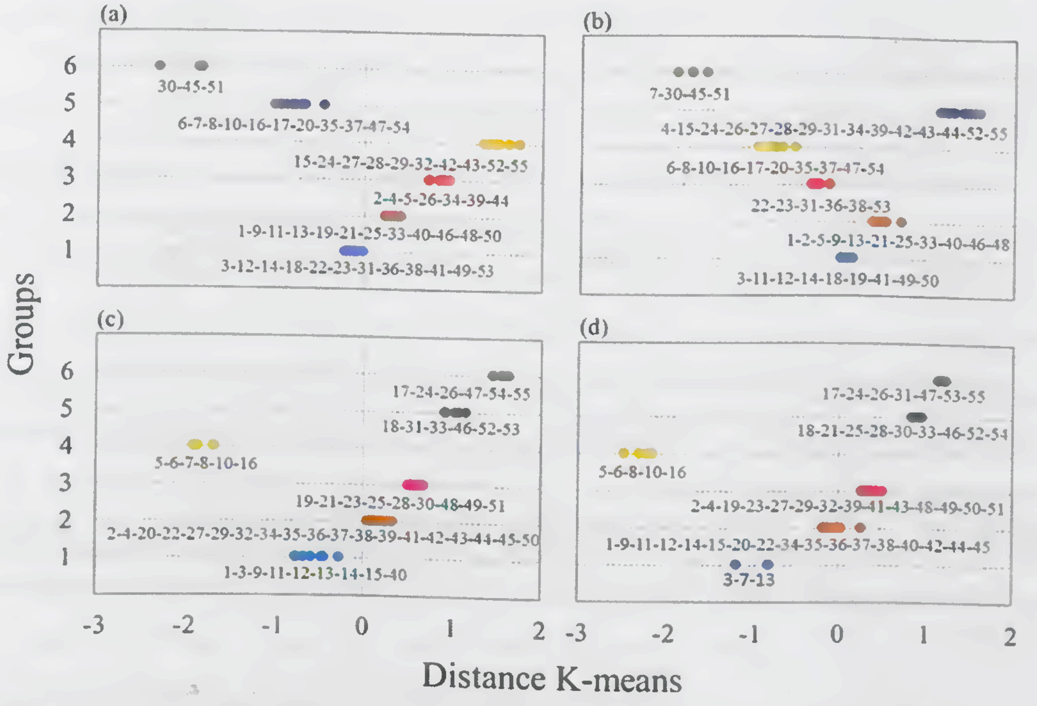

Figure 6. K-means distance for groups of similar performances (GSP) formed by10-day period temperature (a), monthly temperature (b), 10-day period rainfall (c) and monthly rainfall (d) in the Brazilian Amazon. The values indicate the locations of the surface meteorological stations according to Figure 1.

In order to estimate T_{SUR} values by ECMWF we determined that GSP 4 had the best results observed with $R^2 = 0.66$ and $d = 0.89$ (Figure 7(d)). The lowest values were in GSP 6, with $R^2 = 0.10$ and $d = 0.32$ (Figure 7(f)) on 10-day period scale, as well as for the monthly models, with $R^2 = 0.0621$ and $d = 0.21$ (Figure 8(f)). This variability is due to meso and macro climatic influences, such as surface moisture, air masses and mainly by the influence of ITCZ, what was reinforced by Delahaye et al. (2015).

Monthly LRA presented better perforamance (R^2) on GSPs 1, 2 and 5 (Figure 8(a), (b) and (e)).

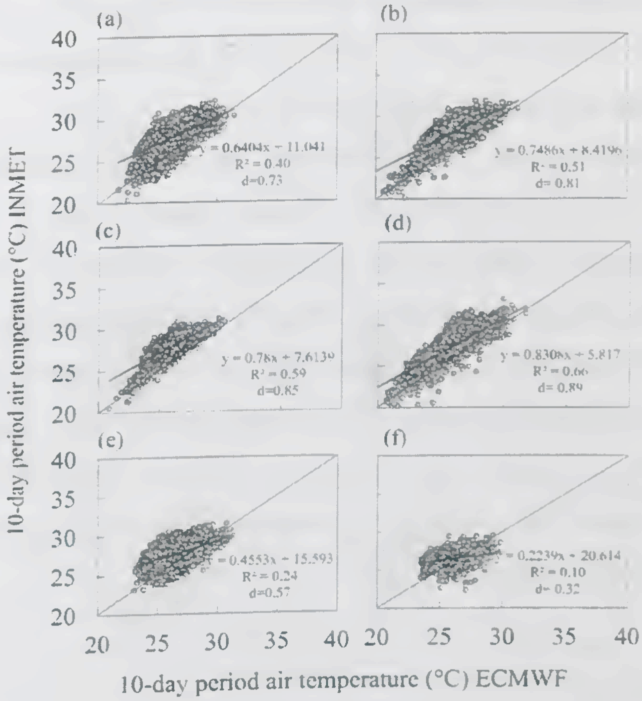

Figure 7. Decent adjustments for surface temperature estimates (INMET) from grid data of the ECMWF general circulation model for performance GSPs in the Brazilian Amazon. GSP 1 (a), GSP 2 (b), GSP 3 (c), GSP 4 (d), GSP 5 (e) and GSP 6 (f).

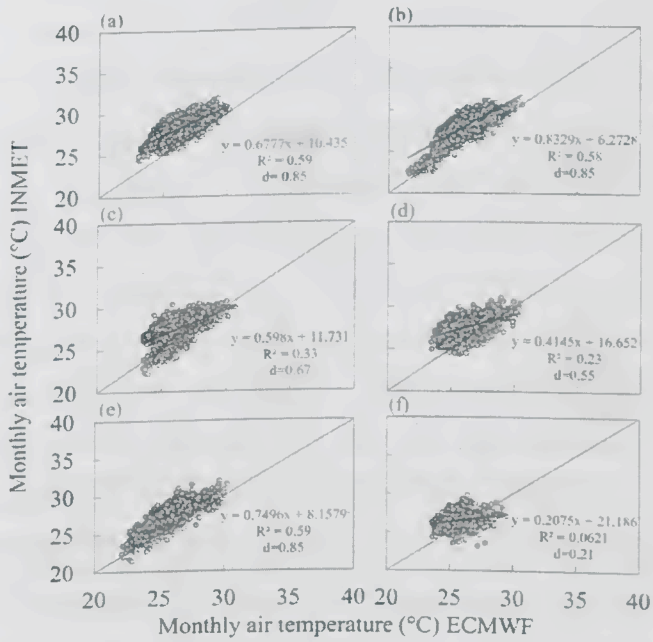

Figure 8. Monthly adjustments for surface temperature estimates (INMET) from grid data of the ECMWF general circulation model for performance GSPs in the Brazilian Amazon. GSP 1 (a), GSP 2 (b), GSP 3 (c), GSP 4 (d), GSP 5 (e) and GSP 6 (f).

P is the most affected seasonal variable in the Brazilian Amazon. In order to obtain this information about the variation of P, the parameters of the Fourier series were adjusted representing the P_{ECMWF} data.

We observed that for the adjustments of P, the monthly scale had a greater precision and accuracy than on 10-day period scale. In GSPs 6 and 4, for 10-day period and monthly scales, we find the adjustments with the highest and the lowest accuracies, respectively. The R^2 obtained in GSP 6 on a 10-day period scale is 0.63 and d = 0.87 (Figure 9(f)) and for a monthly period scale R^2 = 0.76 and d = 0.93 (Figure 10(f)). In the adjustments with lower accuracy as analyzed in GSP 4, values of R^2 and d for a 10-day period scale were respectively 0.13 and 0.36 (Figure 9(d)) and for a monthly scale R^2 = 0.21 and d= 0.52 (Figure 10(d)), respectively.

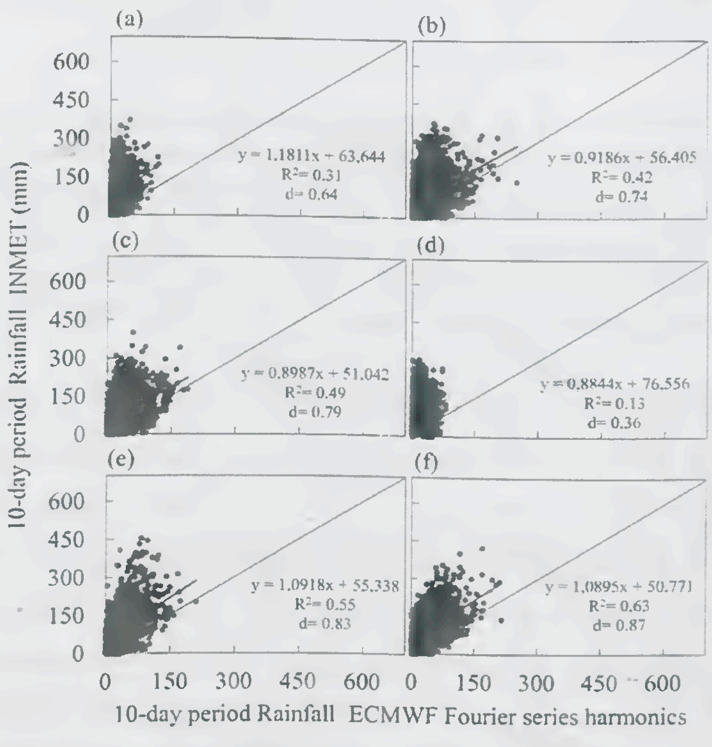

Figure 9. 10-day period models for INMET rainfall estimates by ECMWF stations adjusted by the Fourier series for performance GSPs in the Brazilian Amazon. GSP 1 (a), GSP 2 (b), GSP 3 (c), GSP 4 (d), GSP 5 (e) and GSP 6 (f).

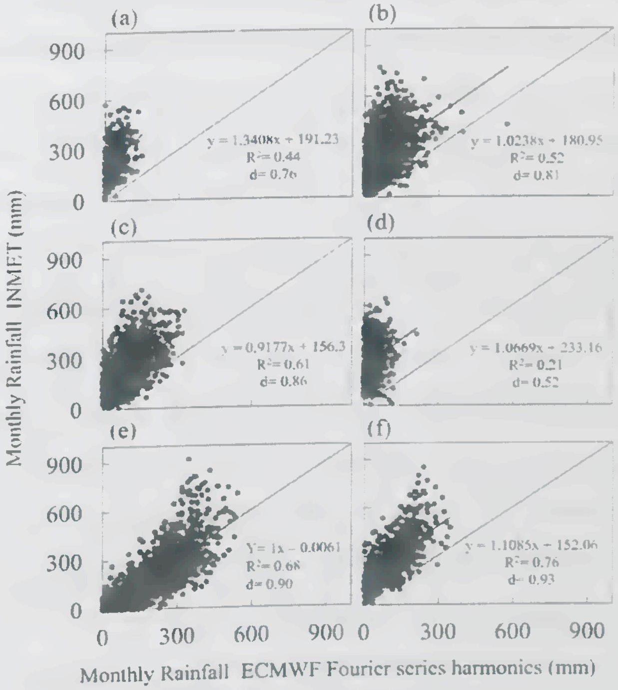

Figure 10. Monthly models for estimates of surface rainfall (INMET) from grid data by the ECMWF model adjusted by the Fourier series for performance GSPs in the Brazilian Amazon. GSP 1 (a), GSP 2 (b), GSP 3 (c), GSP 4 (d), GSP 5 (e) and GSP 6 (f).

The Fourier series accurately represented the periodic functions of the MLRs, allowing to evaluate the linear dependence in the time series and characterizing the amplitude of preexisting periodicities and the frequency obtained in the time domain, thus reducing the noises existing in the historical series. Stratifying the analysis of the two main periods (dry and rain) during the year in the Amazon region, we observed that the dynamics of T and P (Figure 11 and 12) follows the same pattern of monthly variation observed in Figure 2. T was underestimated by ECMWF (Figure 11 (a) and (c)) up to 2°C in the drier period when compared to the values of rain season (Figure 11 (b) and (d)).

P_{ECMWF} values are conservative, with less variability when compared to P_{SUR} (Figure 12). The driest periods tend to have lower P_{SUR} values than P_{ECMWF} (Figure 12(a) and(c)) and the inverse situation in the rainy season (Figure 12(b) and (d)), showing that rainfall estimates in the region still require caution when using data from P_{ECMWF}. We emphasize that these estimates should be used to extend the information network of the thermal-water regime in the Amazon and therefore considered of reasonable significance for evaluating the estimated values.

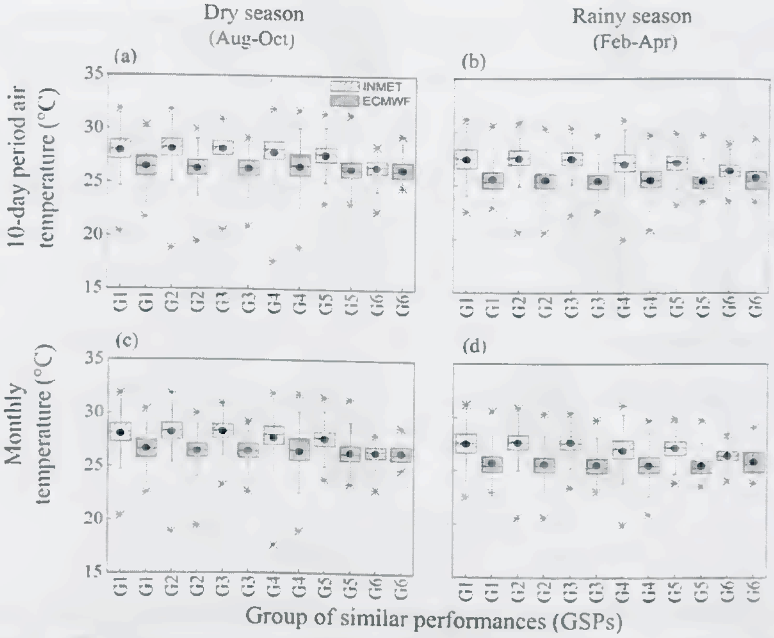

Figure 11. GSP variability of 10-day period air temperature seasons in dry (a) and rainy (b) and monthly (c) and (d) seasons.

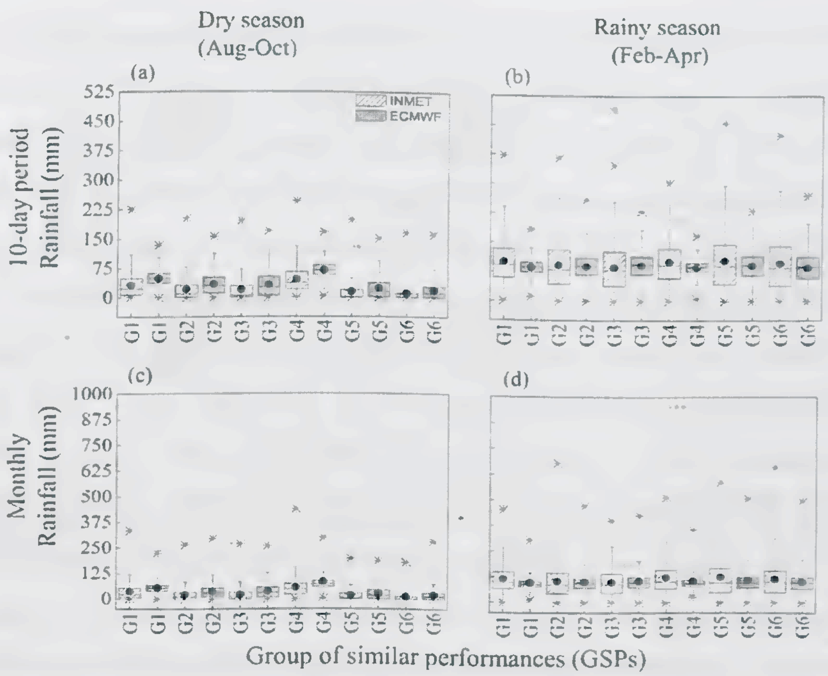

Figure 12. GSP variability of 10-day period rainfall seasons in dry (a) and rainy (b) and monthly (c) and (d) seasons.

Fernandes et al. (2008) also concluded that there is an underestimation of ECMWF for rainfall during the wet season in the Amazon basin and an overestimation during the dry season in comparison to the Global Precipitation Climatology Project (GPCP-Version 2) and to the Global Land Precipitation by the Climate Prediction Center (CPC).

With the Dickey-Fuller test we evaluated that all the observations among the GSPs do not follow a particular distribution, thus presenting a steady effect with p value less than 0.05. The trend analyzed in the different seasons (dry and rainy) among rainfall GSPs indicated variability between INMET and ECMWF, with no effect of decreasing or increasing trend over time (Figure 13).

In GSPs 1 and 4 the precision and accuracy of the data were the lowest comparing the dry and rainy seasons. In the dry period, R^2 in GSP 1 and 4 was 0.22 and 0.16 and d = 0.53 and 0.43 (Figure 13A, G) respectively. In the period of larger rainfall supply R^2 was equal to 0.15 and 0.21, for GSP 1 and 4, respectively.

The P_{ECMWF} data in the dry period had a greater trend than P_{SUR}. This reinforces the claim that ECMWF data tend to overestimate those of INMET in the dry period. In the rainy season there is alternation of major and minor trends in the time series between the GSPs, however the INMET variations are more pronounced, with rain amplitudes close to 170 mm (Figure 13 (j) and (l)). However, the observations do not present significant differences for the groups evaluated.

This result is consistent with the findings of Almeida et al. (2017), who observed that for 47 stations throughout the Brazilian Legal Amazon on the period between 1973–2013, most of the stations did not present significant trend for rainfall, neither for annual nor seasonal series.

Satyamurty et al. (2010) analyzed the annual and seasonal trend of rainfall in 18 stations along the major rivers of the Brazilian Amazon Basin, using data from at least 45 years and observed that the region shows an insignificant and weak downward trend and therefore, found no significant trends for most cases, except for a few individual stations.

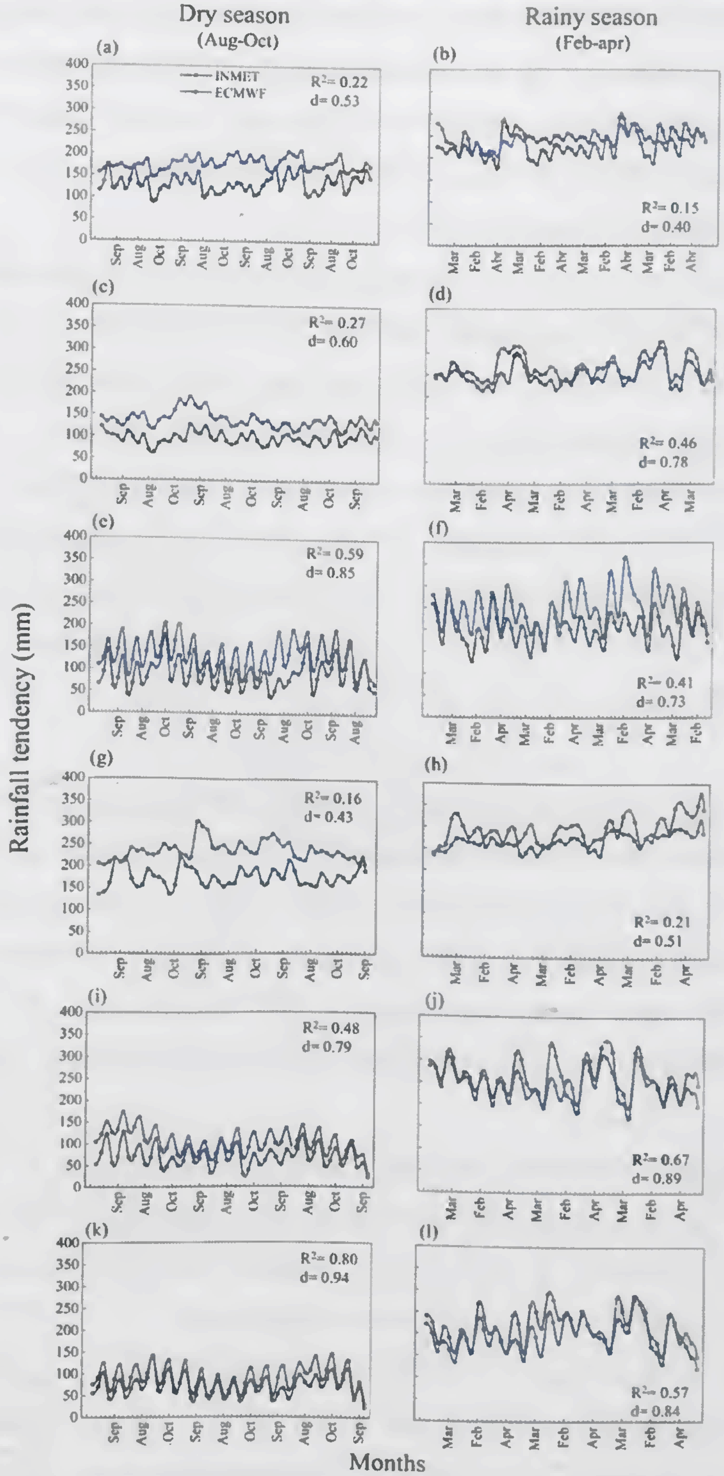

Figure 13. Trend analysis by the Dickey-Fuller test of monthly precipitation by GSPs of stations in the Brazilian Amazon in the dry and rainy season. GSP 1 (a and b), GSP 2 (c and d), GSP 3 (e and f), GSP 4 (g and h), GSP 5 (I and j) and GSP 6 (k and l).

The analysis of the frequency by Fourier series among the GSPs showed that there is a predominance of extreme periods of high and low rainfall in the Brazilian Amazon for every 17 to 22 10-day period corresponding to 5 to 7 months. GSPs 4, 5 and 6 showed the same frequency with 17 10-day period (Figure 14, (d), (e), and (f)). However, GSPs 1, 2 and 3 predominated their frequencies at 22, 19 and 20 10-day period (Figure 14 (b) and (c)) respectively.

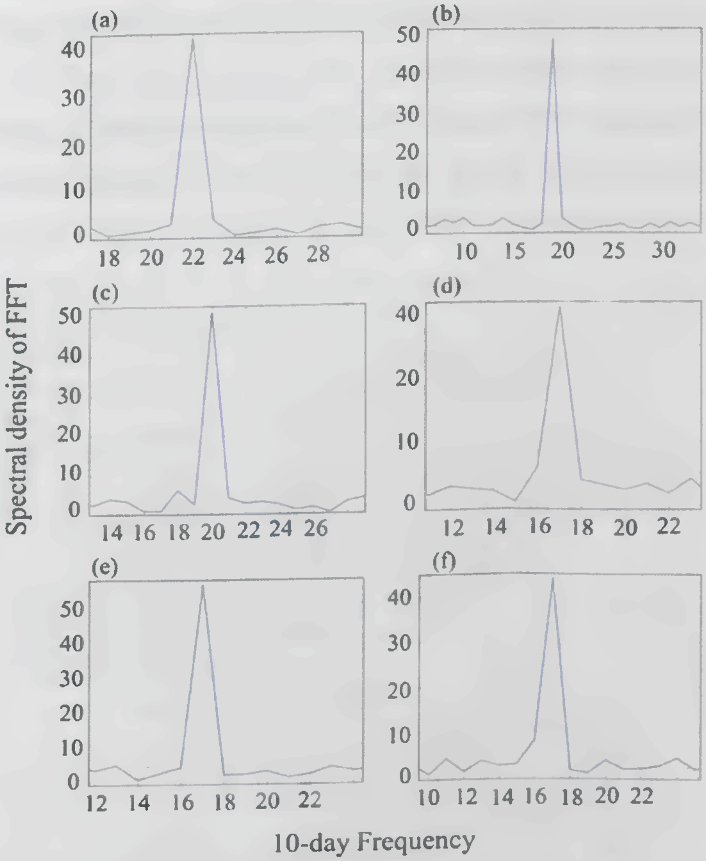

Figure 14. Rain Fourier Frequency among Station GSPs. GSP1 (a), GSP 2(b), GSP 3(c), GSP 4(d), GSP 5(e) e GSP 6(f).

The R^2 of several models among the GSPs were interpolated by the IDW method, being possible to identify accuracies for different regions of the Brazilian Amazon (Figure 15 and 16).

The pattern of variation of the thermal amplitude in the Brazilian Amazon, characterizing small variations in amplitude at different times of the year among the GSPs, from the ECMWF and INMET data (Figure 11, 12), reflect the spatial distribution of the sites and interpolation of the accuracy values of R^2 of T (Figure 15), characterizing them by spatially non-homogeneous areas.

GSPs as a function of 10-day period and monthly T (Figure 15(a) and (b)) are generally not located in the same region. A small part of the southern, northern and northeastern regions of the Brazilian Amazon had R^2 above 0.70, with the values being mainly GSPs 3 and 4 on the 10-day period scale and 5 and 1 on the monthly scale, which extends its range of interpolation above 0.60 and 0.70, shifting from the south of the region along the northwest and north of the Brazilian Amazon (Figure 15 (b)).

The comparison of the two monthly analyzes below, in synthesis, allows us to conclude that the small variability in T is reflected on spatially not homogeneous areas between GSPs and R^2 values.

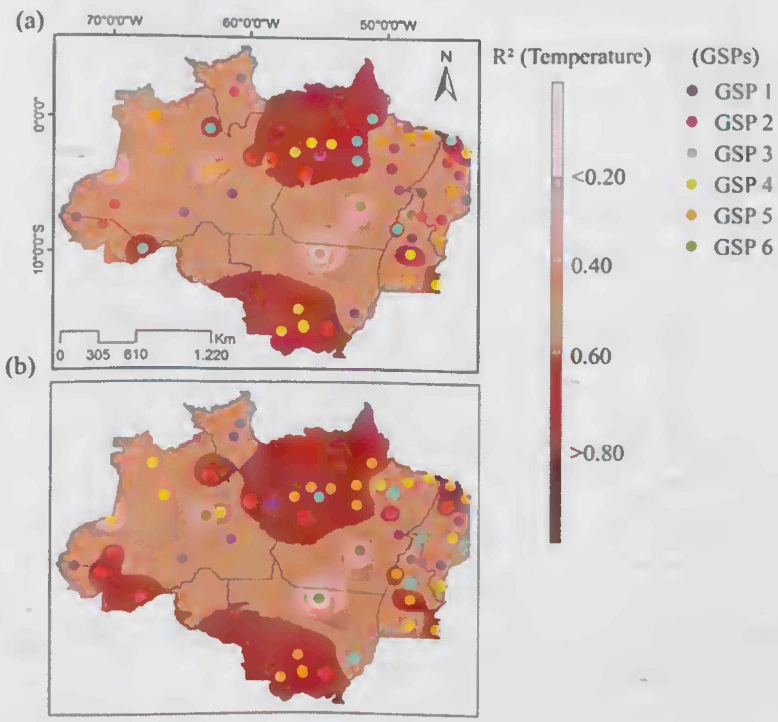

Figure 15. Interpolation of R^2 and spatialization of GSPs in the Brazilian Amazon for 10-day period (a) and monthly (b) temperatures.

Different from T, that presents small variations, P in the Brazilian Amazon has great variability. This variability among the regions generated a good relation for the characterization of GSPs and interpolated R^2 values.

The 10-day period values of P as observed in Figure 16A tend to have smaller precisions (R^2) than the monthly ones (Figure 16(b)). However, the distribution of GSPs in the interpolated areas did not present any distinction. The homogeneous bands of R^2 with values between 0.55 to 0.66 in the 10-day period scale and greater than 0.74 in the monthly scale, are more present in the south of the region towards the northeast coast, indicating in these areas the GSPs 3,5 and 6 (Figure 16 (a) and (b)), respectively.

From the north to the southwest coast the values of R^2 ranged from 0.55 to 0.34 for a 10-day period scale and 0.60 to 0.70 for a monthly scale. The northwest of the Brazilian Amazon is characterized as the region of less precision among the adjusted models, with values lower than 0.40 both 10-day period and monthly (GSP 4).

These results assist us in making better decisions, as regards to the best model of adjustment of global stations by the surface, already presented and discussed in the figures 6,7,8 and 9.

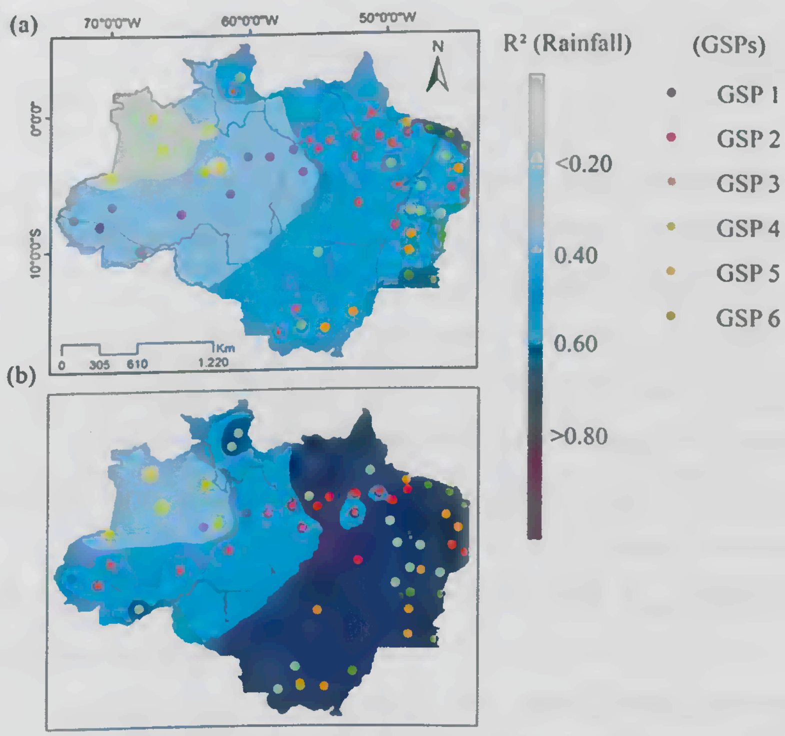

Figure 16. Interpolation of R^2 and spatialization of GSPs in the Brazilian Amazon for 10-day period rainfall (a) and monthly (b) rainfall.

Betts and Viterbo (2005) attributes that part of this inter annual variability in the runoff estimated by the ECMWF is related to problems with atmospheric moisture analysis. In the rainy season, convection over the Amazon is sensitive to processes at many temporal and spatial scales because the boundary layer is close to neutrality in terms of moisture (Betts et al., 2009). If not suppressed by cloud cover, large daytime surface evaporation generates convective instability and strong convective daytime cycle, which are sensitive to dynamic forcing at broader scales (Betts et al., 2009;Van Heerwaarden et al., 2010; Tawfik and Dirmeyer, 2014).

Therefore, Itterly et al. (2016) points out that during the rainy season the atmosphere is very close to saturation and therefore very unstable concerning water vapor fluxes, indicating a statistically significant connection among convective intensity, diurnal cycle and atmospheric state. As a result, forecast and climate models differ in their earth-surface-boundary layer and cloud couplings.

2.4 Conclusions

The adjustment of the surface data with the ECMWF data for T and P, on10-day period and monthly scales, had a high performance in the northeastern part of the Amazon.

The variability of temperature and precipitation in the Amazon modulated the north and northwestern part more humid than the southern part. For all the studied variables, the calibrations that had satisfactory temperature responses were in the southern and northern parts of the Amazon and for rainfall in the south of the region, towards the northeast coast.

The northwest of the Amazon, influenced mainly by the Inter tropical Convergence Zone and the convective environment of that region, presented low performance of the calibration models.

Fourier series is a good tool for modeling a very large amount of precipitation data, mitigating the problems arising from large variability that is characteristic of a large data set, describing the periodic components (regime) and trends. In the Brazilian Amazon there is a tendency of greater values of rain from every 5 to 7 months.

The proposed ECMWF calibration methodology presented overestimation and underestimation in some regions of the Amazon and can be used for estimates of temperature and rainfall for a 10-day period and for a monthly period to represent these surface data in the Brazilian Amazon, provided that they are calibrated.

The temperature and precipitation data from the ECMWF reduce the dependence of surface meteorological data, expanding the database used in climatic prognoses, besides presenting high spatial representativity, free of charge and easy access, facilitating practical applications such as ecological, agriculture, meteorology, among others.

2.5 References

ALESSANDRINI, S.; SPERATI, S.; PINSON, P. A. Comparison between the ECMWF and COSMO Ensemble Prediction Systems applied to shortterm wind power forecasting on real data. **Applied Energy**. v.107, p. 271–280, 2013. Avaiable in: < http:// doi.org/10.1016/j.apenergy.2013.02.041>

ALMEIDA, C.T.; OLIVEIRA JÚNIOR, J.F.; DELGADO, R.C.; CUBO, P.; RAMOS, M.C. Spatiotemporal rainfall and temperature trends throughout the Brazilian Legal Amazon, v1973–2013. **International Journal of Climatology**, v. 37, n. 4, p. 2013-2026, 2017. Avaiable in: < http://doi: 10.1002/joc.4831>

BECHTOLD, P.; CHABOUREAU, P.; BELJAARS, A.; BETTS, A. K.; KOHLER, M.; MILLER, M.; REDELSPERGER, J. The simulation of the diurnal cycle of convective precipitation over land in a global model. **Quarterly Journal of the Royal Meteorological Society**, v. 130, n. 604, p. 3119-3137, 2004. doi: 10.1256/qj.03.103. Avaiable in: < http:// doi:10.3894/JAMES.2010.2.6.>

BETTS, A.K.; DIAS, M. A. F. S. Progress in Understanding Land-Surface-Atmosphere Coupling from LBA Research. **Journal of Advances in Modeling Earth Systems**, v. 2, n. 2, 2010.

BETTS AK, FISCH G, VON RANDOW C, SILVA DIAS CMAF, COHEN JCP, SILVA R, D. R. FITZJARRALD R. The Amazonian boundary layer and mesoscale circulations. Amazonia and Global Change. **Journal of Geophysical Research: Atmospheres**, v. 186, p. 163–181. 2009.

BETTS, A. K.; JAKOB, C. Evaluation of the diurnal cycle of precipitation, surface thermodynamics, and surface fluxes in the ECMWF model using LBA data. **Journal of Geophysical Research: Atmospheres**, v. 107, n. D20, 2002. Avaiable in: < http://doi:10.1029/2001JD000427>

BETTS, A. K.; VITERBO, P. Land-surface, boundary layer, and cloud-field coupling over the southwestern Amazon in ERA-40. **Journal of Geophysical Research: Atmospheres**, v. 110, n. D14, 2005. Avaiable in: < http://doi:10.1029/2004JD005702>

CALLÈDE, J.G.; COCHONNEAU, F.; VIEIRA, A. J. L.; GUYOT, V.; SANTOS, G.; OLIVEIRA, E. The River Amazon water contribution to the Atlantic Ocean. **J. Water Sci.**, v. 23, n. 3, p. 247–273, 2010.

CAVALCANTI, I. F. A.; MARENGO, J.A.; ALVES, L. M.; COSTA, D.F. On the opposite relation between extreme precipitation over west Amazon and southeastern Brazil: observations and model simulations. **Int. J. Climatol**, 2016. Avaiable in: < http://doi:10.1002/joc.4942>

CEGLAR, A.; TORETI, A.; LECERF, R.; VELDE, M. V.; DENTENER, F. Impact of meteorological drivers on regional inter-annual crop yield variability in France. **Agric. For Meteorol.**, v. 216, p. 58–67, 2016. Avaiable in: < http://doi.org/10.1016/j.agrformet.2015.10.004>

CHENG, H.; SINHA, A.; CRUZ, F. W.; WANG, X.; EDWARDS; R. L.; D'HORTA, F. M.; RIBAS, C. C.; VUILLE, M.; STOTT, L. D.; AULER, A. S. Climate change patterns in Amazonia and biodiversity. **Nature Communications**, *v.* 4, p.1411, 2013. Avaiable in: < http://doi: 10.1038/ncomms2415>

CLARA, M. L.; SIMIONATO, C. G.; D'ONOFRIO, E.; FIORE, M.; MOREIRA, D. Variability of tidal constants in the Río de la Plata estuary associated to the natural cycles of the runoff. **Estuar. Coast. Shelf Sci.**, v. 148, p. 85–96, 2014. Avaiable in: < http://doi.org/10.1016/j.ecss.2014.07.002>

COUTINHO, M. D. L.; LIMA, K. C.; SILVA, C. M. S. Regional climate simulations of the changes in the components of the moisture budget over South America. **Int. J. Climatol.**, v. 36, p. 1170–1183, 2016. Avaiable in: < http:// doi: 10.1002/joc.4411>.

COX, P. M.; HARRIS, P. P.; HUNTINGFORD, C.; BETTS, R. A.; COLLINS, M.; JONES, C. D.; JUPP, T. E.; MARENGO, J. A.; NOBRE, C. A. Increasing risk of Amazonian drought due to decreasing aerosol pollution. **Nature**, v. 453, p. 212–215, 2008. Avaiable in: < http://doi: 10.1038/nature06960>.

DELAHAYE, F., KIRSTETTER, P. E.; DUBREUIL, V.; MACHADO, L. A. T.; VILA, D. A.; CLARK, R. A consistent gauge database for daily rainfall analysis over the Legal Brazilian Amazon. **Journal of Hydrology**, v. 527, p. 292–304, 2015. Avaiable in: < http:// doi.org/10.1016/j.jhydrol.2015.04.012>.

DICKEY, D. A.; FULLER, W. A. Distribution of the estimators for autoregressive time series with a unit root. **Journal of the American Statistical Association**, v. 84, p.427–431, 1979.

DOUGHTY, C. E.; LOARIE, S. R.; FIELD, C. B. Theoretical impact of changing albedo on precipitation at the southernmost boundary of the ITCZ in South America. **Earth Interact,** v. 16, p.1–14, 2012. Avaiable in: < http:// dx.doi.org/10.1175/2012EI422.1>.

DRUMOND, A.; MARENGO, J. A.; AMBRIZZI, T.; NIETO, R.; MOREIRA, L.; GIMENO, L. The role of the Amazon Basin moisture in the atmospheric branch of the hydrological cycle: a Lagrangian analysis. **Hydrol. Earth Syst. Sci**. v. 18,p. 2577–2598, 2014. Avaiable in: < http:// dx.doi/10.5194/hess-18-2577>.

Elshorbagy, A.; Simonovic, S. P.; Panu, U. S. Noise reduction in chaotic hydrologic time series: facts and doubts. **J. Hydrol.**, v. 256, p. 147–165, 2002. Avaiable in: < http:// dx.doi.org/10.1016/S0022-1694(01)00534-0>.

ESPINOZA, J. C.; GUYOT, J. L.; RONCHAIL, J.; COCHONNEAU, G.; FILIZOLA, N.; FRAIZY, P.; LABAT, D.; OLIVEIRA, E.; JULIO ORDONEZ, J.; VAUCHEL, P. Contrasting regional dischargeevolutions in theAmazonbasin (1974–2004). **J. Hydrol.**, v. 375, p. 297–311, 2009a. Avaiable in: < http:// dx.doi/10.1016/j.jhydrol.2009.03.004>.

ESPINOZA, J. C.; RONCHAIL; J.; GUYOT, J. L.; COCHONNEAU, G.; NAZIANO, F.; LAVADO, W.; OLIVEIRA, E.; POMBOSA, R.; VAUCHEL, P. Spatio-temporal rainfallvariability in theAmazonbasin countries (Brazil, Peru, Bolivia, Colombia, andEcuador). **Int. J. Climatol.**, v. 29, p. 1574–1594, 2009b. Avaiable in: < http:// dx.doi/ 10.1002/joc.1791>.

FERNANDES, K.; FU, R.; BETTS, A. K. How well does the ERA40 surface water budget compare to observations in the Amazon River basin?,**J. Geophys. Res.**, v. 113, n. D11117, 2008. Avaiabel in: < http:// dx. doi:10.1029/2007JD009220>.

GLOOR, M. R. J. W.; BRIENEN, D.; GALBRAITH, T. R.; FELDPAUSCH, J.; SCHÖNGART, W.; GUYOT, J. L.; ESPINOZA, J. C.; LLOYD, J.; PHILLIPS, O. L. Intensification of the Amazon hydrological cycle over the last two decades. **Geophys. Res. Lett.**, v. 40, p. 1729–1733, 2013. Avaiable in: < http:// dx. Doi/ 10.1002/grl.50377>.

HARMAN, B. I.; KOSEOGLU, H.; YIGIT, C. O. Performance evaluation of IDW, Kriging and multiquadric interpolation methods in producing noise mapping: A case study at the city of Isparta, Turkey. **Applied Acoustics**, *v.* 112, p.147–157, 2016. Avaiable in: < http:// dx. doi:org/10.1016/j.apacoust. 2016.05.024>.

HOAGLIN, D.; WELSCH, R. The hat matrix in regression and ANOVA. **Am Stat**, v. 32, p. 17-22, 1978.

ITTERLY, K. F.; TAYLOR, P. C.; DODSON, J. B.; TAWFIK, A. B. On the sensitivity of the diurnal cycle in the Amazon to convective intensity. **J. Geophys. Res. Atmos.**, v. 121, p.8186–8208, 2016. Avaiable in: < http:// dx. doi:10.1002/2016JD025039>.

JAIN, A. K.; MURTY, M. N.; FLYNN, P. J. Data Clustering: A Review. **ACM Computing Surveys**, v. **31**, p. 264-323, 1999.

LAGUARDIA, G. Representing the precipitation regime by means of Fourier series. **Int. J. Climatol.,** v.31, p.1398–1407, 2011. Disponivel em: < http:// dx.doi: 10.1002/joc.2169>.

LEE, T.; OUARDA, T. Long-term prediction of precipitation and hydrologic extremes with nonstationary oscillation processes. **J. Geophys. Res. Atmos.**, v. 115, n. D13, 2010.

LIEBMANN, B.; MARENGO, J. A. Interannual Variability of the Rainy Season and Rainfall in the Brazilian Amazon Basin. **J. Climate**, *v.* 14, p.4308–4318, 2001. Avaiable in: < http://dx.doi:org/10.1175/1520-0442(2001)014<4308:ivotrs>.

LIN, Y. H.; LO, M. H.; CHOU, C. Potential negative effects of groundwater dynamics on dry season convection in the Amazon River basin. **ClimDyn.,** v. 46, p. 1001–1013, 2016. Avaiable in: < http:// dx.doi/ 10.1007/s00382-015-2628-8.

LIU, G.; GUO, Z. A clustering-based differential evolution with random-based sampling and Gaussian sampling. **Neurocomputing**, *v.* 205, p. 229–246, 2016. Avaiable in: < http:// dx.doi.org/10.1016/j.neucom.2016.04.040.

MACKINNON, J. G. Critical Values for Cointegration Tests. **Queen's Economics Department Working Paper**, *v.* **1227**, p.1-19, 2010.

MARENGO, J.; NOBRE, C. Clima da regiaoAmazonica, in: Tempo e clima no Brasil, Cavalcanti, I. F. A. (ed.), **Oficina de Textos**, Sao Paulo, Brazil, p.197–212, 2009.

MARENGO, J. A.; ESPINOZA, J. C. Extreme seasonal droughts and floods in Amazonia: causes, trends and impacts. **Int. J. Climatol**., v. 36, p. 1033–1050, 2016. Avaiable in: < http:// dx.doi: 10.1002/joc.4420>.

MARENGO, J. A. Interannual variability of surface climate in the Amazon basin. **Int. J. Climatol.**, v. 12,p. 853–863, 1992.

MARENGO, J. A. Characteristics and spatio-temporal variability of the Amazon River Basin Water Budget. **Climate Dynamics**, v. 24, p. 11–22, 2005. Avaiable in: < http:// dx.doi:10.1007/s00382-004-0461-6>.

MARTHA, G. B. J.; Contini, E; Navarro, Z. **Caracterização da Amazônia Legal e macrotendências do ambiente externo**. Embrapa Estudos e Capacitação: Brasília, DF, 2011.

MORAES, J.R.S.C.; ROLIM, G.S.; APARECIDO, L.E.O. 2017. Software for the detection of outliers and influential points based on the HAT method. **Aust J CropSci**. v.11, p. 459-463, 2017. Avaiable in: < http:// dxdoi: 10.21475/ajcs.17.11.04.356>.

OLITA, A.; RIBOTTI, A.; SORGENTE, R.; FAZIOLI, L.; PERILLI, A. SLA-chlorophyll-a 519 variability and covariability in the Algero-Provençal Basin (1997–2007) through 520 combined use of EOF and wavelet analysis of satellite data. **Ocean Dyn**. v. 61, p. 89–102, 2011>.

RING, C.; MANNIG, B.; POLLINGER, F.; PAETH, H.Uncertainties in the simulation of precipitation in selected regions of humid and dry climate. **Int. J. Climatol**. v.36, p. 3521–3538, 2016. Avaiable in: < http:// dxdoi: 10.1002/joc.4573>.

SANG, Y.F.; WANG, D.; WU, J.C.; ZHU, Q.P.; WANG, L.The relation between periods' identification and noises in hydrologic series data. **J. Hydrol**. v. 368, p.165–177, 2009.

SATYAMURTY, P.; CASTRO, A.A.; TOTA, J.; GULARTE, L.E.S.; MANZI, A.O. Rainfall trends in the Brazilian Amazon Basin in the past eight decades. Theor. Appl. Climatol. v.99, p.139–148,2010. Avaiable in: < http:// dxdoi: 10.1007/s00704-009-0133-x>.

SAWASKE, S.R.; FREYBERG, D.L. An analysis of trends in baseflow recession and lowflows in rain-dominated coastal streams of the pacific coast. **J. Hydrol**. v.519: 599–610, 2014. Avaiable in: < http:// dx doi.org/10.1016/j.jhydrol.2014.07.046>.

SYPKA, P.; KUCZAB, J.; STARZAKB, R. Assumptions for Fourier-based modelling of diurnal temperature variations in the top soil layer under Istebna spruce stands. **Agric For Meteorol**.v.222, p.71–86,2016. Avaiable in: < http:// dxdoi.org/10.1016/j.agrformet.2016.03.004>.

TANAKA, M.O.; FERNANDES, J.D.F.; SUGA, C.M.; HANAI, F.Y.; SOUZA, A.L.T.D. Abrupt change of a stream ecosystem function along a sugarcance-forest transition: integrating riparian and in-stream characteristics. **Agric. Ecosyst. Environ**. v.207, p.171–177, 2015. Avaiable in: < http:// dx doi.org/10.1016/j.agee.2015.04.014>.

TAWFIK, A.B.; DIRMEYER, P.A. A process-based framework for quantifying the atmospheric preconditioning of surface-triggered convection. **Geophys. Res.** Lett. v.41, p.173–178, 2014. Avaiable in: < http:// dx doi:10.1002/2013GL057984>.

TAYLOR, P.G.; CLEVELAND, C.C.; WIEDER, W.R.; SULLIVAN, B.W.; DOUGHTY, C.E.; DOBROWSKI, S.Z.; TOWNSEND, A.R. Temperature and rainfall interact to control carbon cycling in tropical forests. **Ecol. Lett**. v.20, p. 779–788, 2017. Avaiable in: < http:// dxdoi: 10.1111/ele.12765>.

VAN HEERWAARDEN, C.C.; ARELLANO, J.V.G.; TEULING, A.J. Land-atmosphere coupling explains the link between pan evaporation and actual evapotranspiration trends in a changing climate. **Geophys. Res. Lett**.v. 37 L21401,2010. Avaiable in: < http:// dxdoi:10.1029/2010GL045374>.

WERTH, D.; AVISSAR, R. The local and global effects of Amazon deforestation. **J Geophys. Res**. v.**107**, p. 8087, 2002. Avaiable in: < http:// dxdoi:10.1029/2001JD000717>.

WILLIAMS, E.; ROSENFELD, D.; MADDEN, N.; GERLACH, J.; GEARS, N.; ATKINSON, L.; DUNNEMANN, N.; FROSTROM, G.; ANTONIO, M.; BIAZON, B.; CAMARGO, R.; FRANCA, H.; GOMES, A.; LIMA, M.; MACHADO, R.; MANHAES, S.; NACHTIGALL, L.; PIVA, H.; QUINTILIANO, W.; MACHADO, L.; ARTAXO, P.; ROBERTS, G.; RENNO, N.; BLAKESLEE, R.; BAILEY, J.; BOCCIPPIO, D.; BETTS, A.; WOLFF, D.; ROY, B.; HALVERSON, J.; RICKENBACH, T.; FUENTES, J.; AVELINO, E.Contrastingconvective regimes over theAmazon: Implications for cloud electrification. **J. Geophys. Res.** v.**107**(D20), p.1-50,2002. Avaiable in: < http:// dxdoi: 10.1029/2001JD000380>.

WILLMOTT, C.J.; ACKLESON, S.G.; DAVIS, R.E.; FEDDEMA, J.J.; KLINK, K.M.; LEGATES, D.R.; O'DONNELL, J.; ROWE, C.M.Statistics for evaluation and comparison of models. **Journal of J. Geophys. Res**. v.90 (C5), p.8995-9005, 1985. Avaiable in: < http:// dx doi:10.1029/JC090iC05p08995>.

XIE, Y.; HUANG, Q.; CHANG, J.; LIU, S.; WANG, Y. Period analysis of hydrologic series through moving-window correlation analysis method. **J. Hydrometeorol**.v. 538, p.278–292,2016. Avaiable in: < http:// dxdoi.org/10.1016/j.jhydrol.2016.04.024>.

YANG, C.G.; LIN, Z.H.; YU, Z.B.; HAO, Z.C.; LIU, S.F. Analysis and simulation of human activity impact on streamflow in the huaihe river basin with a largescale hydrologic model. **J. Hydrometeorol**. v. 11, p. 810–821, 2010. Avaiable in: < http:// dx doi.org/10.1175/2009JHM1145.1>.

CAPÍTULO 3 - AGROMETEOROLOGICAL MODELS TO FORECAST AÇAI PRODUCTION IN IRRIGATED AND UNIRRIGATED SYSTEMS

Abstract

The increasing demand in Brazil and the world for products derived from the Açai palm (açai or assai) (*Euterpe oleracea* Mart) has created changes in the processes involved in açai production systems, principally with respect to the use of precocious varietals, expansion of plantations into non-irrigated areas, and also due to the necessity of maintaining production in situations of seasonality and climate fluctuation. The objective of this study was to estimate acai fruit productivity in irrigated system (IRRS) and rainfed system or unirrigated (RAINF) using agrometeorological models in response to climate conditions in the principal acai producing region in Brazil. Modeling was done using multiple linear regression using the "stepwise forward" method of variable selection. Monthly air temperature values (T), solar radiation (SR), vapor pressure deficit (VPD), precipitation + irrigation (P+I), and potential evapotranspiration (PET) in six phenological phases were correlated with production. The thermal necessity value was calculated through the sum of accumulated degree days (ADD) up to the formation of fruit clusters, as well as the time necessary for initial leaf development, using a temperature base of 10°C. The most important meteorological variables were T, SR, and VPD for IRRS, and for RAINF water stress had the greatest effect. The phase of leaf maturation and emission of the spathe, for both IRRS and RAINF, were the variables that were most sensitive to climate conditions. The thermal sum for the initiation of leaf formation was approximately 750 °C accumulated in a year, while for initial leaf development up to fruit harvest it was 8.350 °C. The greatest fruit production occurred in November and December in each cultivation system, and production ranged from 7.500 kg ha^{-1} in the RAINF to 16.500 kg ha^{-1} in the IRRS. The accuracy of the agrometeorological models, using maximum values for average absolute percent error (MAPE), was 0.01 in the IRRS and 1.12 in the RAINF. Using these models production was predicted approximately 6 to 9 months before the harvest, in April, May, November, and December in

the IRRS, and January, May, June, August, September, and November for the RAINF.

Keywords: amazon, *Euterpe oleracea,* crop model, ECMWF, multiple linear regression, NASA Power.

3.1 Introduction

The State of Pará has the largest area in the world cultivated with the acai palm (*Euterpe oleracea* Mart.), and produces about 60% of acai fruit in Brazil. The principal product derived from the acai fruit is a processed pulp for which, beginning in 2002, demand increased worldwide, and this increase created a necessity to increase acai production in Pará (HOMMA and SANTANA, 2009).

Acai production systems have been greatly modified during recent years due to expansion of cultivation into areas of solid ground (*terra firme*) with the use of irrigation systems (FARIAS NETO et al., 2011). However, the supply of acai has continued to be below the demand on a global market level. Acai production is strongly related to climate conditions and soil water availability, and in intensively managed and irrigated acai plantations in the largest acai production areas of Pará increases in growth, development, and productivity have been obtained during the last few years, but there is still a great need for studies that relate climate variables to productivity.

According to Ferraz (1999) and Bergamaschi (2007), the phenology of a healthy plant directly depends on favorable meteorological conditions for strong growth, development, and productivity. In this context, variables such as rainfall, air temperature, solar radiation, and vapor pressure deficit can influence the dynamics of pollinating insects and fruit predators, with climate having a strong influence during periods of flowering, fruiting, and leaf senescence (PEDRONI et al., 2002). Therefore, studies that aim to characterize phenologic states are important in order to understand and explain plant population dynamics (SPINA et al., 2001) associated to climate and soil conditions in a specific region (FOURNIER, 1974).

Oliveira et al (2002) related that when peach palm (*Bactris gasipaes* Kunth) is subjected to soil water stress, leaf water potential is reduced as soil water stress increases. These authors observed that water stress in this palm triggered responses such as reduction in stomatal conductance and transpiration rates, accompanied by water potential reductions in leaves. Stomatal conductance was reduced by 54% and transpiration decreased by 31% when leaf water potential was near -1.5 MPa. Photosynthesis was reduced by 40% by the sixth day of water stress, and leaf water potential was -1.6 MPa.

In the literature available on this subject there are studies of the type described in the current work that have been done for several palm species cultivated under conditions similar to those of the Amazon, but none for the acai palm. For example, Nkodo et al. (2016) related that wind speed, potential evapotranspiration, maximum air temperature, and vapor pressure deficit explained 60% of the variation in oil palm production (*Elaeis guineensis*). Urrego et al (2016) evaluated the reproductive phenology of buriti (*Mauritia flexuosa*) and showed that short-live climatic fluctuations influenced flowering and fruiting patterns, including mortality, recruitment, and establishment of seedlings.

Ruiz and Alencar (2004) reported that for the patauá palm (*Oenocarpus bataua*) the phenologic state when “fruits fall from the fruit clusters” presented a positive correlation with insolation, maximum and average temperatures, and a negative correlation with rainfall and relative humidity, but for other phenologic states meteorological variables had no influence.

Agrometeorological models can aid in the decision-making process in order to predict production in agricultural systems. However, for palms, such models have been reported only for oil palm. Keong & Keng (2012) described a quantitative relationship through time between meteorological variables and fruit clusters, relating that abortion of inflorescences and sex differentiation are influenced by soil water status, having a latency period between 9 and 11 and 22 and 23 months before harvest, respectively, while Hutha et al. (2014)

adequately simulated productivity in different management systems and were able to predict future crop responses to management techniques including fertilizer applications.

In this context, the objective of this work was to predict the productivity of acai fruits in irrigated and unirrigated systems using. agrometeorological models calibrated for different phonological states.

3.2 Material and Methods

Açai palm productivity data from 2003 to 2012 were collected in commercial production areas with 5 x 5 m spacing for a total of 500 stems/ha.

Two management systems in Tomé-Açu, Pará were analyzed: Irrigated system (IRRS) and rainfed system or unirrigated (RAINF). This municipality is located in the northeast of the State of Pará and it is one of the largest production areas in the State. The climate is classified in the Köppen system as Af_3 (without a defined dry period and with the month with the least rainfall having more than 60 mm), and according to the method in Martorano et al. (1993), is similar to the climate type of the northwest region of the western Amazon (Figure 1).

For each acai stem, the total mass of fruits, number of fruit clusters, and average mass of 100 fruits were collected on a monthly basis beginning in the second semester of 2006 when the plants were approximately 3.5 years old.

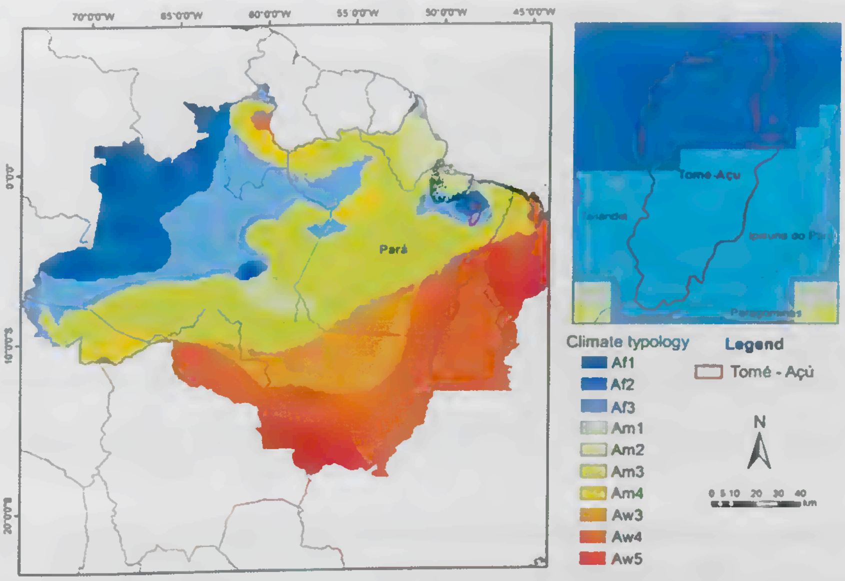

Figure 1. Climate classification map for the Amazon basin highlighting the region of Tomé-Açu, Pará, using data from Martorano et al. (1993).

Data for rainfall (P) from 2000 to 2012 was obtained from the National Water Agency (ANA). The data for maximum (TMAX), minimum (TMIN), and average (T= (TMAX+TMIN)/2) air temperatures, Solar radiation (SR), and potential evapotranspiration (PET) were estimated using the system of the European Centre for Medium Range Weather Forecasts (ECMWF) with a spatial resolution of 27 x 27 km (longitude x latitude). The software ENVI was used to extract the values of TMAX, TMIN and SR, for the study site. Daily relative humidity (RH) was obtained based on the NASA/POWER system.

Vapor pressure deficit data for the study area were used to estimate atmospheric hydrological demand by using the difference between vapor pressure saturation and vapor partial pressure (Eq. 1 to 3).

$$VPD = Es - Ea \qquad (1)$$

$$Es = 6.11 \times 10^{\left(\frac{7.5 \times TMED}{237.3 + TMED}\right)} \qquad (2)$$

$$Ea = \frac{RH \times Es}{100} \qquad (3)$$

where, VPD= vapor pressure deficit (kPa); Es = vapor pressure saturation (kPa); Ea = vapor partial pressure (kPa); RH= Relative humidity (%); T= average air temperature (°C).

Data for real evapotranspiration (ETA) were estimated using the sequential hydrologic balance model as proposed by Thornthwaite and Mather (1955) with capacity of available water (CAW) equal to 125 mm. For the IRRS system daily precipitation and irrigation was used (P+I). In this system, irrigation in the experimental area was conducted daily and replaced water lost through ETA.

The time series trend was derived through linear adjustment as proposed by Gujarati and Porter (2011) in order to visualize other components capable of influencing production as a function of climate effects on the production of fruits per stem (kg $stem^{-1}$). Productivity was estimated using the average production of fruits per stem multiplied by the number of plants per hectare in each cultivation system.

Six phenological states were considered in this research and are described as follows: (1) sprouting and initial development of leaves (SIDL); (2) mature leaves (ML), that are sheathed by other leaves; (3) old leaves (OL), the most external leaf that surrounds the initial development of the spathe; (4) emisson of the spathe (ES); (5) inflorescence and flowering (IF); (6) fruiting and ripening (FR). These events take, on average, 18 months (Oliveira, 2002) in order to harvest every mature fruit cluster of a stem (Figure 2). The stem produces during all months of the year, therefore the phenological states are overlapped with respect to each spathe and leaf being formed.

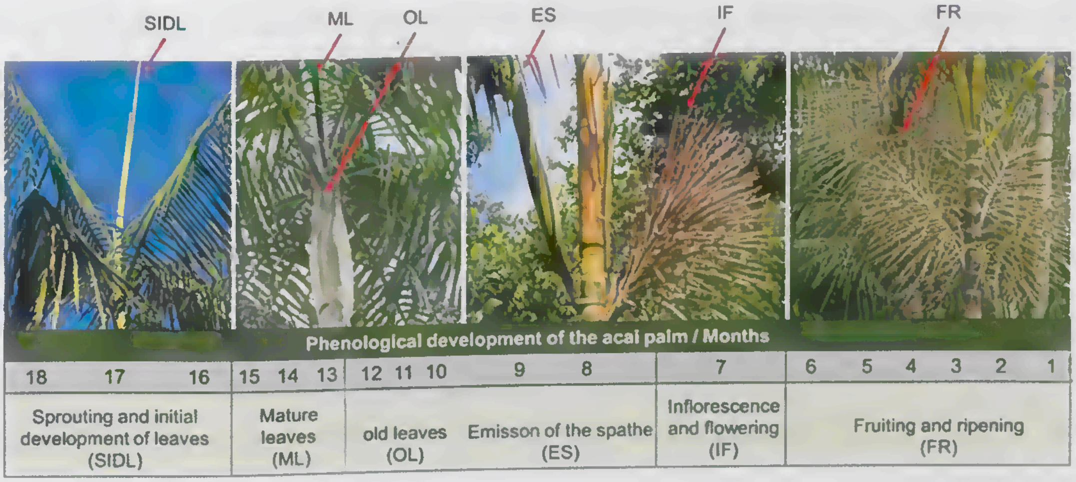

Figure 2. Phenological development of the acai palm (*Euterpe oleracea* Mart.), adapted from Oliveira (2002). The numbers indicate the number of months before harvest of each fruit cluster.

Thermal necessity data were calculated using the sum of accumulated degree-days (ADD) (eq. 2), up to the complete formation of fruit clusters, as well as the time passed since the initial development of the leaf. ADD values for the complete formation of fruit clusters were calculated for the period from 18 months before harvest up to the final maturation phase of the plant. For initial leaf formation, ADD values were calculated for the period from 18 months before harvest.

$$\sum ADD = \left\{\frac{[Tmax+Tmin]}{2}\right\} - Tbase \qquad (2)$$

where, ∑ADD = the sum of accumulated degree-days; Tmax = maximum daily air temperature (°C); Tmin = minimum daily air temperature (°C); Tbase = base temperature of the crop, considered equal to 10 °C due to its similarity to other palms (Zaid and de Wet, 2017).

In order to evaluate the accumulated ADD, all harvests of fruit clusters during the period of this study were included, taking into consideration the stems with average production, which totaled five. Each progeny is represented by 10 stems with their respective production, totaling 990 ADD evaluations per cluster/stem/progeny combination.

Using the duration of each phenological phases and that of the complete production cycle, an analysis was conducted to see if there was a correlation between monthly production of each stem and the agrometeorological variables separated into phenological phases by cluster analysis. This analysis

This analysis allowed for understanding of the influence of each meteorological variable in each stage of development on productivity in the two management systems. In the IRRS the analysis was made based on T, SR, P+I, PET and VPD. In the RAINF water stress (WS), T, SR and VPD were used, with all variables always analyzed beginning 18 months before the harvest of fruit clusters.

A monthly linear correlation analysis was conducted using these same meteorological variables for each of the management systems in an attempt to map their influence during the entire cycle of the plants.

Modeling was done using multiple linear regression in each management system using the “stepwise forward” method of variable selection. This procedure iteratively constructs a sequence of regression models through addition of variables at each step. The criteria for addition or removal of variables at any step is done through an F-test, with the factor loads being subsequently estimated in order to evaluate the variables that best explain the model.

In order to explain the efficiency of the adjustment of the predictive model the average absolute percent error (MAPE) was used (Eq. 3), and precision was measured by the coefficient of determination (adjusted R^2) (Eq. 4), and the measurement of tendency for systematic error (ES) (eq. 5)

$$MAPE(\%) = \frac{\sum_{i=1}^{N}([Yesti - Yobsi/Yobsi] \times 100)}{N} \qquad (3)$$

The MAPE expresses the general accuracy of the model;, Yesti, the estimated value; Yobsi, the observed value; and N corresponds to the total number of observations.

$$R^2 ajustado = \left[-1 \frac{(1-R^2)\times(N-1)}{N-K-1}\right] \quad (4)$$

In equation 4, R^2 is the coefficient of determination (sum of squares of the regression / total sum of squares), and k is the number of independent variables.

$$ES = \sqrt{\frac{\sum_{i=1}^{N}(Yobs-\hat{Y})^2}{N}} \quad (5)$$

In equation 5, $\hat{Y}$ is the average estimated Y.

3.3 Results and Discussion

The municipality of Tomé-Açu has a climate seasonality that is characteristic of the Amazon, divided into rainy and less-rainy periods that, in certain months, can have deficits of water availability intense enough that allow these months to be classified as a period of dry season that is typical of nearby regions. The most intense rainfall (P) occurs in the months of February to May, with values above 350 mm, and the least amount of rainfall occurs between July and September, with values below 50 mm (Figure 3.a).

During the study period the T of the region was 25.5°C, and the TMAX had its highest annual amplitude of 27.7 °C and 32.3°C, in April and October, respectively. The thermal amplitude of TMIN varied about 1°C, with values ranging from 21.8°C in July to 22.7 °C in November (Figure 3.a).

Between the months of July and November the soil presented water deficiency (WS), with the largest deficits (about 75 mm) in September and October (Figure 3.b). In contrast, between December and May there was an excess of water in the soil, with averages above 100 mm.

October was the month with the lowest values for relative humidity (RH) with values near 82%, and the largest values of SR with 22.5 MJ m^{-2} day^{-1}. In contrast, in April the RH reached values above 90%, and SR was near 15 MJ m^{-2} day^{-1} (Figure 3.c), emphasizing that in this period the atmosphere is much more cloudy due to the presence of the Intertropical Convergence Zone (Martorano et al., 2017)

The VPD and PET are variables that are directly related and that follow the same pattern of monthly variation, with lower values in April and greater ones in September and October (Figure 3.d).

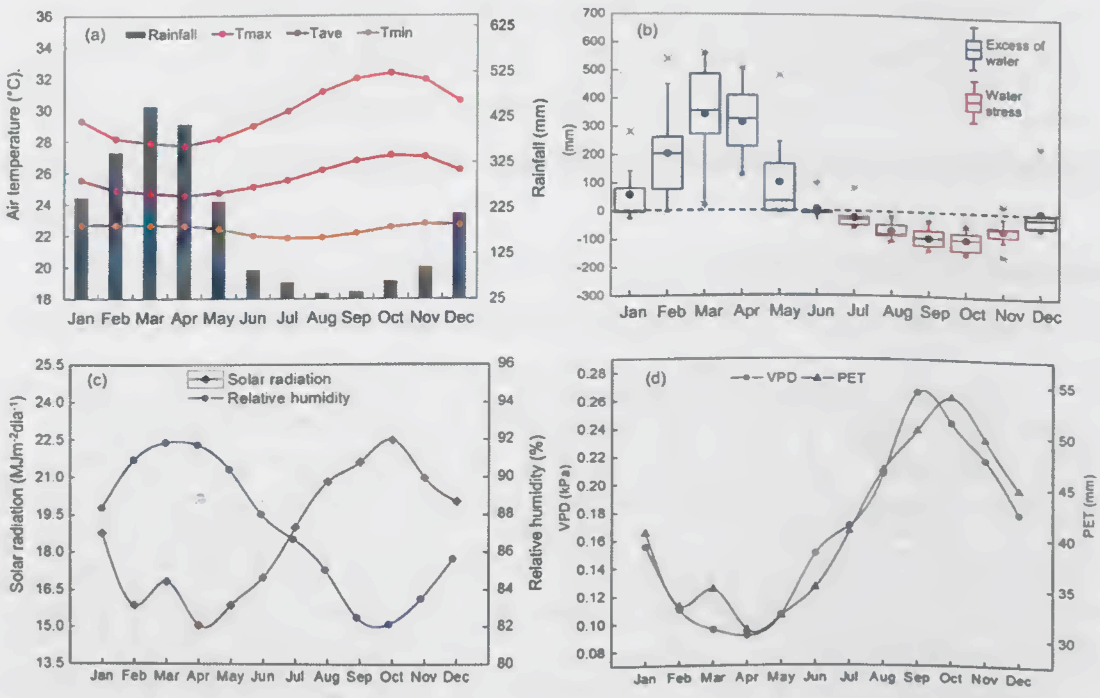

Figure 3. Average values for meteorological variables in the region of Tomé-Açu during the study period in two acai management systems: a) monthly rainfall (mm), maximum, average, and minimum temperatures (°C); b) hydrologic balance (mm); c) relative humidity (%) and global solar radiation (MJ m^{-2} day^{-1}); d) vapor pressure deficit VPD (KPa) and Potential Evapotranspiration– PET (mm).

With respect to irrigated acai (IRRS), the average value for production of fruit was 16,500 kg ha^{-1}, while in the RAINF the average value was 7,500 kgha^{-1} with a difference of 9,000 kg ha^{-1} between the systems. Greater production per stem was registered in the months of November and December in both systems, with average values ranging from 4.03 kg and 1.2 kg in November, and 4.72 kg and 1.5 kg in December in the IRRS and RAINF, respectively. The number of fruit clusters harvested per plant were also greatest during these months with average values ranging from 1.2 to 1.3 in the IRRS and 0.6 to 0.8 in the RAINF (Figure 4.a, b).

August and September had the lowest production per stem with the lowest number of fruit clusters and fruit mass in the IRRS; in the RAINF these values were lowest from June to September. Venturieri (2015) related that there is a correlation between rainfall, nectar production, pollen availability, and stigma receptivity. Therefore, the low production values during these months could be related to stages of inflorescence and flowering since, during February and March the high rainfall could have made insect visits to flowers difficult, which consequently would impact fertilization of the flowers.

Another element that could influence flower production is variation in air temperature. In C3 plants such as the acai palm photorespiration rates can be as dynamic as those for photosynthesis (SCHULZE et al., 2016), being altered by light, CO_2 concentration, and air temperature (ZHOU et al., 2016). Therefore, photorespiration rates increase with an increase in light intensity and temperature (WINGLER et al., 1997). In this situation a plant will reduce photosynthesis and increase photorespiration, which will have a direct and significant effect on plant growth (HEINEKE, 2001). It is estimated that average temperatures between 28 and 30 °C or higher tend to reduce photosynthetic rates (KERBAUY, 2008).

In the Tomé-Açú region, between August and November, TMAX was above 30 °C (Figure 3.a), indicating that the acai stems could have been experiencing thermal stress during the period of these maximums. These elevated temperatures could reduce the production of fruit clusters from March to May thus causing low fruit production per stem. However, when the fruit cluster is forming, principally in the RAINF system which experiences soil water limitation, the average fruit mass per cluster is the highest for the entire sampling period, probably due to the high availability of energy (light) and water in the soil due to favorable conditions for development and ripening of the acai fruit (Figure 4.a).

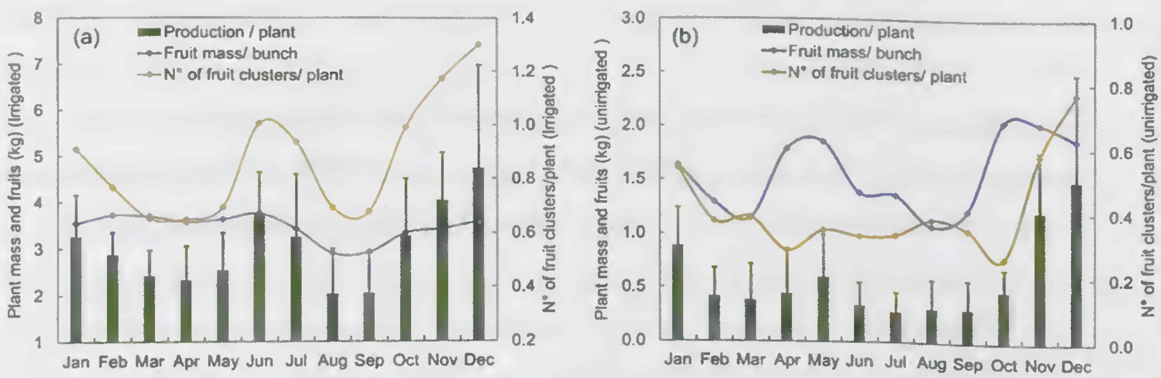

Figure 4. Monthly average for fruit production per stem, fruit mass per cluster, and number of clusters harvested in the Irrigated system a) and rainfed system b). Bars indicate sample standard deviation.

The thermal sum for the initial formation of leaves (SIDL) was about 750 °C accumulated for the year and varied greatly among the progenies, with an average dispersion of 35 days. From this it is inferred that the stems that did not sprout or fully develop leaves during this interval did so afterward (Figure 5).

From the initial development of the leaf up to the harvest of the cluster the thermal sum was, on average, 8,350 °C accumulated during the period for clusters/stems/progenies evaluated, with an average dispersion varying between 8,250 to 8,450 °C (ADD), with a difference of less than 14 days between ripening and harvest of the cluster (Figure 6).

For the RAINF, the ADD was not counted, due to the fact that the plants were not fully developed, with a large number of plants with no clusters formed due to intense periods of soil water deficiency (CAW=125 mm).

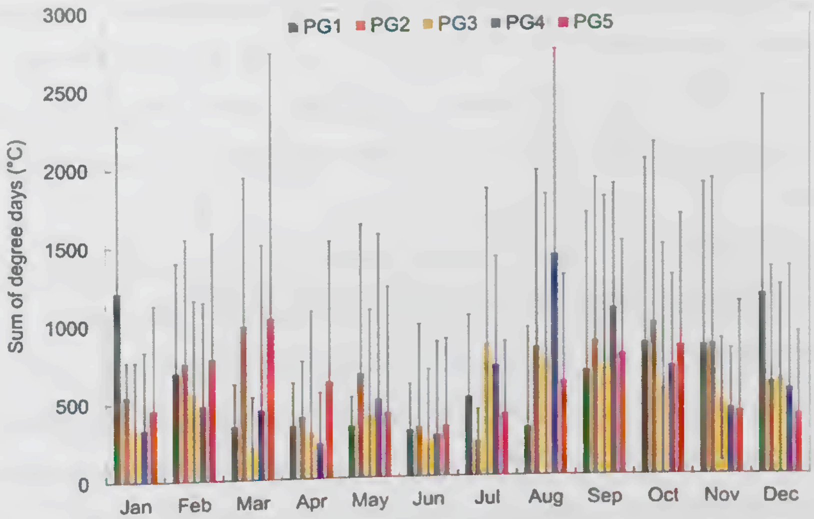

Figure 5. Sum of degree days (°C) for the initial formation of a new leaf after harvest of a cluster in five progenies of acai in an irrigated system in Tomé-Açu, PA. Legend: PG1 to PG5 are the five progenies.

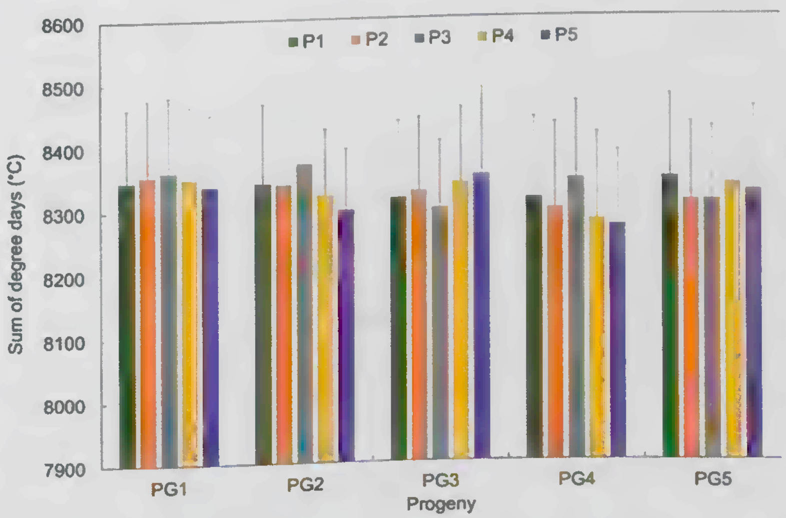

Figure 6. Sum of degree days (°C) for the initial formation of a new leaf after harvest of a cluster in five progenies of acai in an irrigated system in Tomé-Açu, PA. Legend: PG1 to PG5 are the five progenies analyzed with five stems in each progeny.

The principal component (PCA) multivariate analysis (Figure 7) demonstrates the influence of meteorological parameters on fruit productivity based on plant phenological phases. The figure shows that productivity greatly depends on time spent in each phase. The analysis shows that the components

(PC1) and (PC2) explain almost 75% of the total variation in the data. In the IRRS the climatic variables SR, T and VPD during the phases ML and FR positively favor high fruit production per plant and consequently overall productivity (Figure 7a); however, these same variables are inversely related in the EE phase.

In the RAINF, the climatic variable that had the greatest influence on the FR phase was WS, which was directly correlated to productivity. In contrast, SR and T contributed to the ML phase, and P to the OL phase. However, the influence of WS on the phases ES, IF and OL was inversely related to fruit production, as well as for T and SR on the ES phase, showing that phenological phases that precede the FR phase are sensitive to water stress (Figure 7.b).

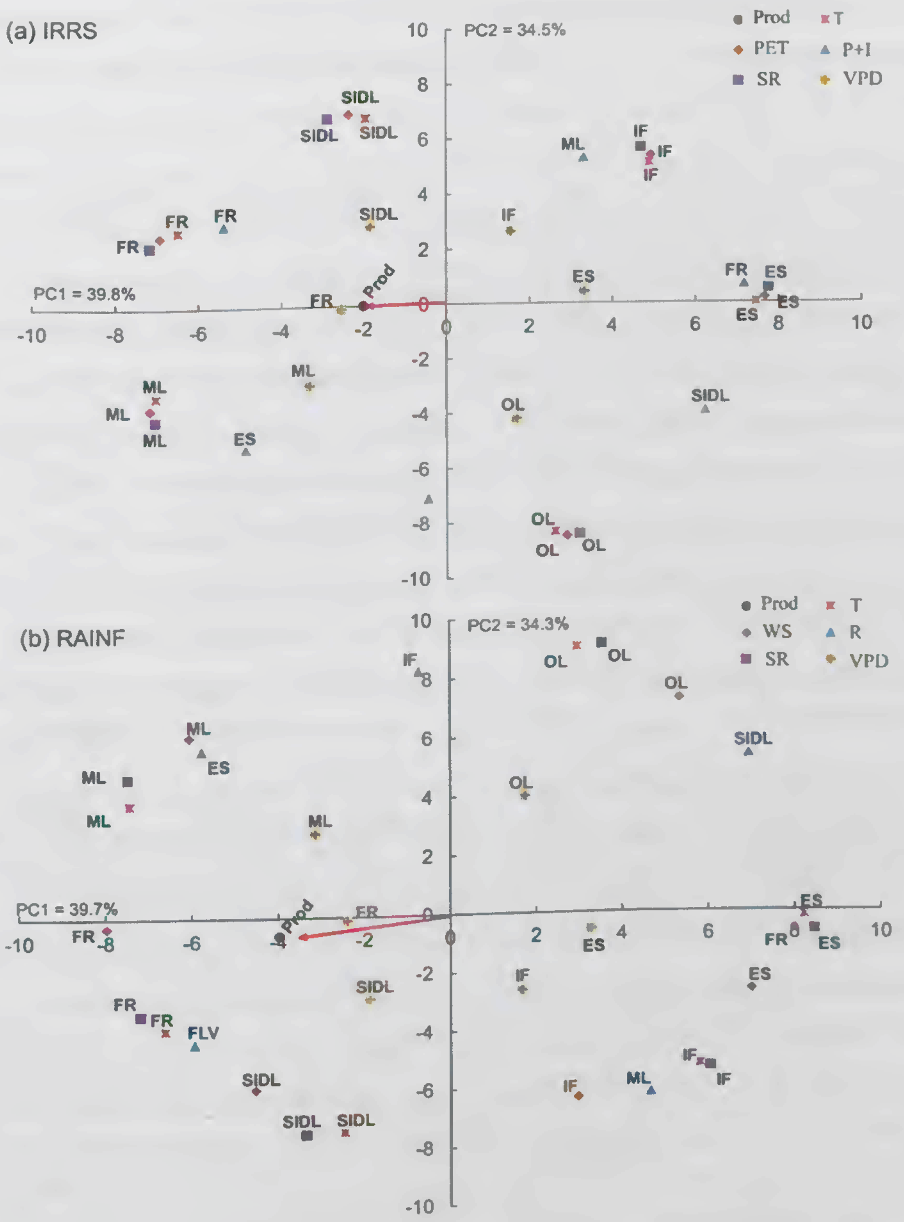

Figure 7. Principal Componente (PCA) biplot of produtivity (Prod) in function of climate in the acai palm irrigated system (IRRS) (a) and rainfed system (RAINF) systems (b), in Tomé-Açu, PA. Legenda: T (average air temperature); PET, (potential evapotranspiration); VPD (vapor pressure deficit); P+I (rainfall and irrigation); SR (global solar radiation); WS (water deficit); P (rainfall). Phenological phases: SIDL (Initial leaf sprouting and development); ML (mature leaf); OL (old leaf); ES (spathe emission); IF (inflorescence and flowering); FR (fruiting and ripening).

Considering the meteorological variables that showed correlations with productivity, in function of phenological phases of the acai palm in the IRRS system, the ES phase was sensitive to agrometeorological conditions (Figure 8.a), principally in the periods of lower production in August and September since the P+I was positively correlated, meaning that the values of these variables increase in function of each other.

However, between April and May, T and RAD had an inverse relationship with production in these phenological phases that occur nine months before the harvest of fruit clusters, during months in which the maximum temperatures occur in Tomé-Açu. In August and September the plants had low production which could possibly be explained by T and SR (Figure 8.d). Marenco and Lopes (2009) discuss the strong effect of T and SR on photorespiration, and for this reason, in conditions of ambient CO_2, photosynthetic efficiency decreases with the increase in these climatic variables.

Another variable that showed an inverse relationship with all plant phenological phases in both the IRRS and RAINF systems, principally during the period of greater production in November and December was VPD . It was expected that as VPD decreased, independent of the phenological phase of the plant during these two months, production would increase thus resulting in larger harvests. Marenco et al. (2014), relate that during the day stomatal conductance quickly responds to the difference in vapor pressure between the leaf and the air, and in general the stomates close as VPD increases (Lloyd et al., 1995, Marenco and Lopes, 2009), thus having a direct effect on photosynthesis.

In the IRRS the WS was the variable that induced the greatest variation in productivity (Figure 9). Therefore, plant productivity will be a function of the phenological phase and the harvest period. For the phenological phases SIDL and OL, during the months of highest average productivity (November and December), WS responded inversely demonstrating that when water deficiency is lower plant production is higher. However, in the FR phase, the plants were directly influenced by increases or decreases in WS, and WS had a direct relationship with IF, principally due to the fact that it occurred during the months with higher rainfall when plant flower fertilization by insects was impeded (VENTURIERI, 2015).

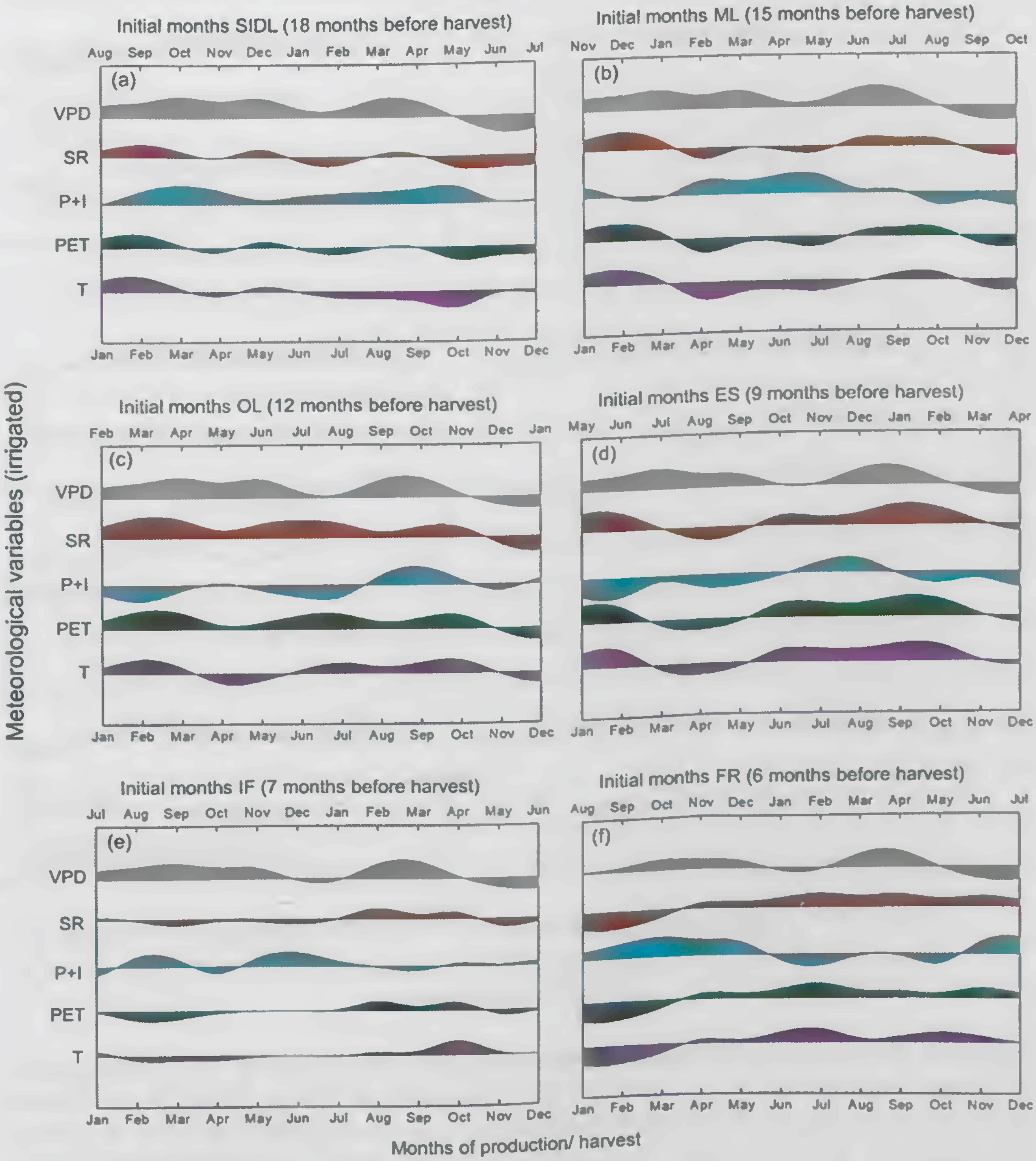

Figure 8. Correlation of meteorological variables with monthly fruit production in the acai palm in Irrigated system (IRRS) in Tomé-Açu, PA in different phenological phases: a) Initial leaf sprouting and development (SIDL); b) mature leaf (ML); c) old leaf (OL); d) spathe emission (ES); e) inflorescence (IF); f) fruiting and ripening (FR).

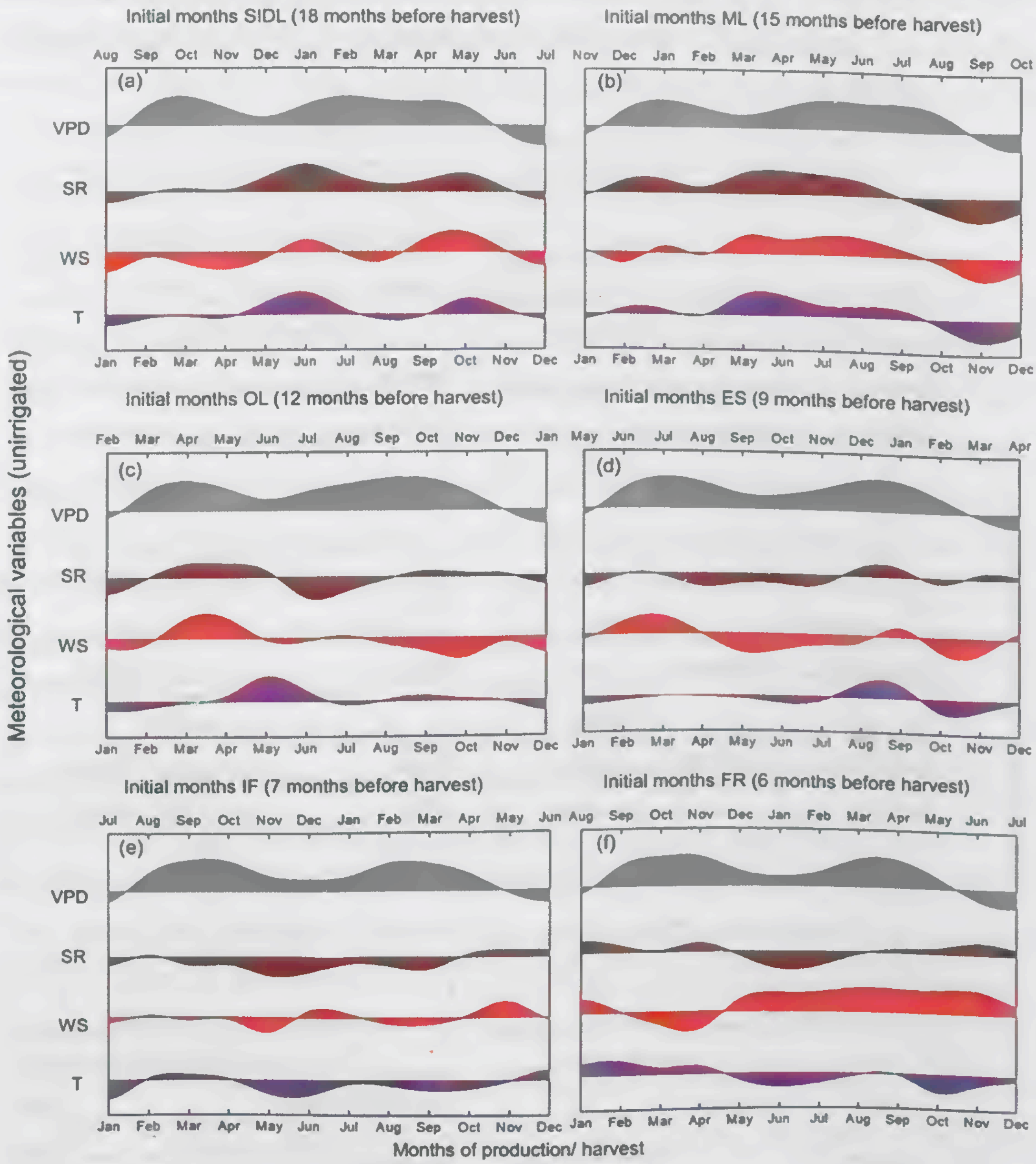

Figure 9. Correlation of meteorological variables with monthly fruit production in the acai palm in rainfed system (RAINF) systems in Tomé-Açu, PA in different phenological phases: a) Initial leaf sprouting and development (SIDL); b) mature leaf (ML); c) old leaf (OL); d) spathe emission (ES); e) inflorescence (IF); f) fruiting and ripening (FR).

The agrometeorological models developed for the months with the highest acai fruit production were all significant for both management systems, with good precision, accuracy, and tendencies. In the IRRS, production was predicted 6 to 9 months before harvest between April, May, November, and

December, and was estimated between the other months. November, and December, months that had high fruit production in the IRRS, had a R^2 greater than 0.95, and a MAPE (%) and ES less than 7.5. For example, the model used to predict production in December used rainfall plus irrigation during the initial leaf sprouting and development phase $P+I_{(SIDL)}$; the vapor pressure deficit during spathe emission $VPD_{(ES)}$; and the $VPD_{(SIDL)}$ with positive angular coefficients for $P+I_{(SIDL)}$ and negative ones for $VPD_{(ES)}$ and $VPD_{(SIDL)}$. In contrast, during the months of lower production, such as in August, the model selected $VPD_{(ML)}$, $P+I_{(SIDL)}$ and $SR_{(FR)}$, with all angular coefficients, being positive for production prediction (Table 1).

Furthermore, as for the IRRS system, the model was able to predict production 6 to 9 months before harvest in January, May, June, August, September, and November. During the months of greatest production of fruits per stem, such as in December, the model considered $WS_{(FVL)}$, $WS_{(SIDL)}$ and $T_{(FR)}$ as the most important climatic variables influencing production during the referenced phenological phases of the plant.

For WS the predictive models were negatively correlated since the limited water supply in the soil led to low fruit production, and positively correlated with T (Table 1). During July, which was the month with the lowest fruit production, the climatic variables that had the greatest influence on phenological phases were $VPD_{(ML)}$, $SR_{(FR)}$ and $WS_{(ES)}$. The model was significant with a p-value less than 0.05, minimum adjusted R^2 of 0.89, MAPE and maximum ES of 21.2 % and 1.76 respectively (Table 1).

Table 1. Models for prediction of production of acai fruits per stem in the irrigated (IRRS) and rainfed (RAINF) system in Tomé-Açu, PA. Legend: T (average air temperature); PET, (potential evapotranspiration); VPD (vapor pressure deficit); P+I (rainfall and irrigation); SR (global solar radiation); WS (water deficit); P (rainfall). Phenological phases: SIDL (Initial leaf sprouting and development); ML (mature leaf); OL (old leaf); ES (spathe emission); IF (inflorescence and flowering); FR (fruiting and ripening).

ths	Irrigated and unirrigated model	p-value	R^2 adj	MAPE(%)	ES
(Jan)	$-0.017 \times PET_{(FR)} + 0.023 \times P{+}I_{(SIDL)} + 0.349 \times T_{(ES)} - 0.2555$	0.001	0.99	0.06	3.36
F (Jan)	$-1.322 \times T_{(IF)} - 0.469 \times T_{(ES)} - 0.157 \times T_{(ML)} + 50.242$	0.001	0.98	1.12	0.94
(Feb)	$-0.001 \times P{+}I_{(OL)} + 0.044 \times PET_{(ES)} + 0.0004 \times P{+}I_{(FR)} - 4.900$	0.002	0.99	0.26	2.90
(Feb)	$2.218 \times VPD_{(FR)} + 0.002 \times WS_{(FR)} - 0.005 \times WS_{(ML)} - 0.469$	0.012	0.99	4.78	0.48
(Mar)	$3.724 \times VPD_{(SIDL)} + 0.0003 \times P{+}I_{(FR)} - 2.250 \times VPD_{(OL)} + 1.038$	0.001	0.99	0.17	2.46
(Mar)	$3.421 \times VPD_{(ES)} - 0.003 \times WS_{(IF)} + 0.001 \times WS_{(FR)} - 0.061$	0.005	0.97	3.64	0.49
(Apr)	$-2.002 \times T_{(ML)} - 0.001 \times P{+}I_{(OL)} + 0.025 \times SR_{(SIDL)} + 51.759$	0.001	0.99	0.01	2.41
(Apr)	$1.715 \times VPD_{(IF)} - 0.188 \times SR_{(ML)} - 0.002 \times WS_{(FR)} + 3.223$	0.005	0.98	3.83	0.57
(May)	$0.004 \times P{+}IR_{(SIDL)} - 0.004 \times P{+}I_{(OL)} + 0.0004 \times PET_{(SIDL)} + 0.310$	0.001	0.99	0.01	2.64
(May)	$4.772 \times T_{(OL)} + 0.005 \times WS_{(ES)} - 0.001 \times WS_{(IF)} - 122.113$	0.010	0.89	7.90	0.60
(Jun)	$-0.004 \times P{+}I_{(FR)} - 4.233 \times T_{(FR)} - 0.006 \times PET_{(IF)} + 118.402$	0.021	0.99	0.08	3.85
F (Jun)	$0.246 \times SR_{(SIDL)} - 0.837 \times SR_{(OL)} + 0.0004 \times WS_{(ES)} + 13.174$	0.001	0.99	2.05	0.39
(Jul)	$-0.006 \times P{+}I_{(FR)} - 2.350 \times SR_{(ES)} - 2.541 \times SR_{(OL)} + 117.782$	0.005	0.99	0.97	3.46
F (Jul)	$3.628 \times VPD_{(ML)} - 0.124 \times SR_{(FR)} + 0.001 \times WS_{(ES)} + 1.796$	0.010	0.98	5.64	0.32
(Aug)	$10.597 \times VPD_{(ML)} + 0.001 \times P{+}I_{(SIDL)} + 0.742 \times SR_{(FR)} - 14.384$	0.041	0.98	1.06	2.20
F (Aug)	$3.046 \times VPD_{(ES)} - 0.161 \times SR_{(ES)} - 0.252 \times T_{(SIDL)} + 9.167$	0.001	0.99	8.61	0.43
(Sep)	$0.007 \times P{+}I_{(OL)} - 0.055 \times PET_{(FR)} - 0.001 \times P{+}I_{(FR)} + 37.971$	0.002	0.98	4.60	2.17
F (Sep)	$1.713 \times VPD_{(OL)} - 0.429 \times SR_{(ML)} + 0.001 \times WS_{(OL)} + 8.576$	0.004	0.98	21.62	0.40
(Oct)	$-6.827 \times T_{(SIDL)} - 0.065 \times PET_{(FR)} + 1.830 \times SR_{(FR)} + 189.291$	0.005	0.99	1.48	3.46
F (Oct)	$-0.007 \times WS_{(OL)} - 0.166 \times SR_{(IF)} - 1.230 \times VPD_{(FR)} + 3.841$	0.041	0.89	14.43	0.52
(Nov)	$-9.751 \times VPD_{(SIDL)} - 2.219 \times SR_{(ML)} + 0.534 \times SR_{(ES)} + 45.674$	0.003	0.98	0.81	4.13
F (Nov)	$-0.004 \times WS_{(ML)} + 0.380 \times WS_{(IF)} - 2.154 \times VPD_{(IF)} + 2.313$	0.006	0.94	6.78	1.33
(Dec)	$0.050 \times P{+}I_{(SIDL)} - 12.678 \times VPD_{(ES)} - 3.994 \times VPD_{(SIDL)} - 10.164$	0.031	0.99	7.26	4.74
F (Dec)	$-0.436 \times WS_{(OL)} - 0.010 \times WS_{(SIDL)} + 2.775 \times T_{(FR)} - 68.307$	0.004	0.91	19.80	1.76

Estimating the factor loads in order to evaluate the variables that best explain the model in December, the month of the largest production in the IRRS system, the variable P+I(SIDL) accounted for 3.8% of the variation, and the variable that least accounted for variation was VPD (0.2%). However, in August, the month with the lowest production, SR(FR) was the variable that most accounted for variation in production (6.4%) (Figurae10.a). In the RAINF system, T(FR) in December, the month of the largest production, was the most important of all meteorological variables. However, July was the month with the lowest average monthly production and had an angular coefficient for SR(FR) of -7.4%, the value that most explained the variation in this model (Figure 10.b).

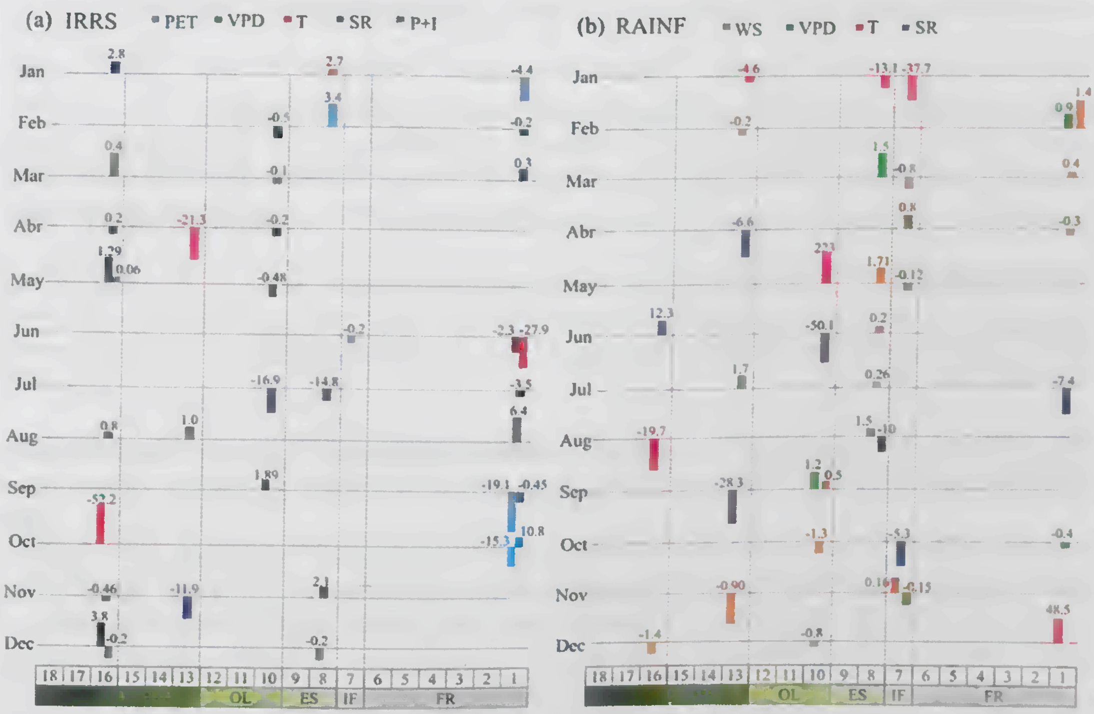

Figure 10. Estimate of the factor loads of monthly agrometeorological productivity models in Acai palm irrigated system (IRRS) (a), and rainfed system (RAINF) (b), in Tomé-Açu, PA. Legenda: T (average air temperature); PET, (potential evapotranspiration); VPD (vapor pressure deficit); P+I (rainfall and irrigation); SR (global solar radiation); WS (water deficit); P (rainfall). Phenological phases: SIDL (Initial leaf sprouting and development); ML (mature leaf); OL (old leaf); ES (spathe emission); IF (inflorescence and flowering); FR (fruiting and ripening).

3.4 Conclusion

The climatic variables evaluated in this study exert distinct influence on the production of Acai fruit in irrigated and unirrigated systems, and consequently on overall production. Air temperature, solar radiation, and vapor pressure deficit are the variables that most influence the productivity of irrigated acai, and soil water deficiency most influences the productivity of in the unirrigated system.

For the both management systems the phenological phases of mature leaves and spathe emission were the most sensitive to climate conditions.

For the months of April, May, November and December in the IRRS, and January, May, June, August, September, and November in the RAINF, the model was able to predict production 6 to 9 months before harvest.

This study showed that it is possible to predict average monthly productivity several months in advance thus aiding in creating strategies for decision-making during the Acai harvest period.

3.5 References

BERGAMASCHI, H. O clima como fator determinante da fenologia das plantas. **CD-ROM**. p. 290-310. 2007.

FARIAS NETO, J.T.; VASCONCELOS, M.A.M.; NOGUEIRA, A.K.M. Produção, processamento e mercado para a cultura do acai: Irrigação. Coleção Cursos Frutal. Semana da Fruticultura, Floricultura e Agroindústria - Frutal Amazônia 2011. Pág. 32 – 40. 2011.

FERRAZ, D. K. Fenologia de árvores em fragmentos de mata em São Paulo, SP. **Revista Brasileira de Biologia**. v.59, n.2, p.305-317, 1999.

FOURNIER, L. A. Um método cuantitativo para la medición de características fenológicas em árboles. **Turrialba**, San Jose, v.24, n.4, p. 422-423, 1974.

GUJARATI, D. N.; PORTER, D. C. Basics Econometrics (5ª Ed.). Publisher **Mcgraw-Hill/Irwin**. 2011.

HEINEKE, D.; BYKOVA, N.; GARDESTROM, P.; BAUWE, H. Metabolic response of potato plants to an antisense reduction of the P-protein of glycine decarboxylase. **Planta**. v. 212, p.880-887. 2001.

HENDERSON, A.; GALEANO, G. Euterpe, Prestoe, and Neonicholsonia (Palmae). **Flora Neotropica**, v. 72, p. 1–89, 1996.

HOMMA, A.K.O.; SANTANA A.C. A agroindústria na Região Norte. In: Zibetti DW & Barroso LA (Eds.) **Agroindústria: uma análise no contexto socioeconômico e jurídico brasileiro**. v.1. São Paulo, LEUD. p.19-43. 2009.

HUTHA, N. I.; BANABASB, M.; NELSON, P. N.; WEBB, M. Development of an oil palm cropping systems model: Lessons learned and future directions. **Environmental Modelling & Software**. v. 62, p. 411–419, 2014.

KEONG, Y. K.; KENG, W. M. Statistical Modeling of Weather-based Yield Forecasting for Young Mature Oil Palm. **APCBEE Procedia** 4: p. 58-65. 2012.

KERBAUY, G.B. Fisiologia vegetal. 2.ed. Rio de Janeiro: **Guanabara Koogan**, 2008. 431p.

LLOYD, J.; FARQUHAR, G.D. The CO2 dependence of photosynthesis, plant growth responses to elevated atmospheric CO2 concentrations and their interaction with soil nutrient status .1. General principles and forest ecosystems. **Functional Ecology**, v. 10, p.4-32.1996.

MARENCO, R. A.; ANTEZANA-VERA, S. A.; GOUVÊA, P. R. S.; CAMARGO, M. A. B.; OLIVEIRA, M. F.; SANTOS, J. K. S. Fisiologia de espécies florestais da Amazônia: fotossíntese, respiração e relações hídricas. **Revista Ceres.** 786-799, 2014.

MARENCO, R. A.; LOPES, N. F. **Fisiologia vegetal: fotossíntese, respiração, relações hídricas e nutrição mineral**. 3ªed. Editora UFV, Viçosa. 486p. 2009.

MARTORANO, L. G.; VITORINO, M. I.; SILVA, B. P. P. C.; MORAES, J. R. S. C.; LISBOA, L. S.; SOTTA, E. D.; REICHARDT, K. Climate conditions in the eastern amazon: Rainfall variability in Belem and indicative of soil water deficit. **African Journal of Agricultural Research**, v. 12(21), p.1801-1810, 2017.

MARTORANO, L. G.; PEREIRA, L. C.; NECHET, D. Tipologia climática do Estado do Pará: adaptação do método de Köppen. **Boletim de Geografia Teorética,** AGETEO-Rio Claro, v. 23, n.45-46, p. 307-312, 1993.

NKODO, F.; PENTANE, N.R.; TABI, F.O. Most responsive periods to climatic factor variations before harvest in oil palm (*Elaeis guineensis* Jacq.) and their quantitative relationships with yields in the coastal zone of Cameroon. **Agric. Biol. J. N. Am.**, p. 70-85, 2016.

OLIVEIRA, M. A. J.; BOVI, M. L. A.; MACHADO, E. C.; GOMES, M. M. A; HABERMANN, G.; RODRIGUES, J. D. Fotossíntese, condutância estomática e transpiração em pupunheira sob deficiência hídrica. **Scientia Agricola**, v.59, n.1, p.59-63. 2002

OLIVEIRA, M. S. P. Biologia Floral do Açaizeiro em Belém, PA. Embrapa Amazônia Oriental. **Boletim de Pesquisa**, nº XX, 26p. 2002.

PEDRONI, F.; SANCHEZ, M.; SANTOS, F. A. M. Fenologia da copaíba (*Copaifera langsdorffii* Desf. - Leguminosae, Caesalpinioideae) em uma floresta semidecídua no sudeste do Brasil. **Revista Brasileira de Botânica**, v.25, n.2, p.183-194, 2002.

RUIZ, R. R.; ALENCAR, J. C. Comportamento fenológico da palmeira patauá (*Oenocarpus bataua*) na Reserva Florestal Adolpho Duke, Manaus, Amazonas, Brasil. **Acta Amazônica**, Manaus, v. 34, n. 4, p. 443-448, 2004.

SCHULZE, S.; WESTHOFF, P.; GOWIK, U. Glycine decarboxylase in C3, C4 and C3–C4 intermediate species. **Plant Biology**, p. 31:29–35, 2016.

SPINA, A. P.; FERREIRA, W. M.; LEITÃO FILHO, H. F. Floração, frutificação e síndromes de dispersão de uma comunidade de floresta de brejo na região de Campinas (SP). **Acta Botânica**, v.15, n.3, p.349-368, 2001.

THORNTHWAITE, C. W.; MATHER, J. R. The water balance. Centerton: Drexel **Institute of Technology, Climatology**. v.8, n.1, p.104, 1955.

URREGO, L. E.; GALEANO, A.; PENUELA, C.; SANCHEZ, M.; TORO, E. Climate-related phenology of Mauritia flexuosa in the Colombian Amazon. **Plant Ecol**. p. 217:1207–1218. 2016.

VENTURIERI, G. R. Ecologia da polinização do açaizeiro (*Euterpe oleracea*) com e sem a introdução de colônias da abelha uruçu-amarela (*melipona flavolineata*). **Dissertação de mestrado**, Universidade Federal de Santa Catarina, SC. 122p. 2015.

WINGLER, A.; LEA, P. J.; LEEGOOD, R. C. Control of photosynthesis in barley plants with reduced activities of glycine decarboxylase. **Planta**. v. 202, p.171-178. 1999.

ZAID, A.; de WET, P.F. Climatic requirements of date palm. **FAO**. Corporate document repository. Acess in 21 july, 2017. http://www.fao.org/docrep/006/Y4360E/y4360e08.htm.

ZHOU, Y.; GRICE, K.; STUART-WILLIAMS, H.; HOCART, C. H.; GESSLER, A.; FARQUHAR, G. D. Hydrogen isotopic differences between C3 and C4 land plant lipids: consequences of compartmentation in C4 photosynthetic chemistry and C3 photorespiration. **Plant, Cell and Environment**. p. 2676–2690. 2016.